Available online at www.sciencedirect.com

ScienceDirect

Geochimica et Cosmochimica Acta 163 (2015) 80–100

Geochimica et Cosmochimica Acta

www.elsevier.com/locate/gca

B, Sr and Pb isotope geochemistry of high-pressure Alpine metaperidotites monitors fluid-mediated element recycling during serpentinite dehydration in subduction mélange (Cima di Gagnone, Swiss Central Alps)

E. Cannaò [a,*], S. Agostini [b], M. Scambelluri [a], S. Tonarini [b], M. Godard [c]

[a] Dipartimento di Scienze della Terra, dell'Ambiente e della Vita, Università di Genova, C.so Europa 26, 16132 Genova, Italy
[b] Istituto Geoscienze e Georisorse, CNR, Via Moruzzi 1, 56124 Pisa, Italy
[c] Geosciences Montpellier, Universite Montpellier 2, Place Eugene Bataillon, 34095 Montpellier, France

Received 9 August 2014; accepted in revised form 14 April 2015; Available online 24 April 2015

Abstract

Tectonic mixing of slab- and mantle-derived materials at the interface between converging plates highly enhances fluid-mediated mass transfer from the slab to the overlying mantle. Subduction mélanges can provide information about the interaction among different slices accreted at plate interface domains, with implications on the tectonic and geochemical evolution of the plate-interface itself. At Cima di Gagnone, pelitic schists and gneiss enclose chlorite harzburgite and garnet peridotite lenses, like in subduction mélanges located in-between downgoing slabs and overlying mantle. These peridotites host MORB-type eclogite and metarodingite, and derive from dehydration of serpentinized mantle protoliths. Their enrichment in fluid-mobile B, As, Sb, U, Th is the result of an early-stage oceanic serpentinization, followed by interaction with host metasediments during subduction burial. Here we define the element exchange process in the Gagnone mélange by means of the B, Sr and Pb isotope analysis of its main lithologies (ultramafic, mafic rocks and paragneiss). The $^{87}Sr/^{86}Sr$ and $^{206}Pb/^{204}Pb$ ratios of ultramafic rocks (0.7090–0.7124 and 18.292–18.837, respectively) show enrichments in radiogenic Sr and Pb after exchange with the host paraschist (up to 0.7287 $^{87}Sr/^{86}Sr$; 18.751 $^{206}Pb/^{204}Pb$). The $\delta^{11}B$ values of peridotites (down to $-10‰$) point to a combined effect of (1) ^{11}B release to deserpentinization fluids (serpentinized protoliths likely had positive $\delta^{11}B$ and lower radiogenic Sr, Pb), and of (2) exchange with fluids from the surrounding metasediments. The whole Gagnone rock-suite is finally overprinted by retrograde fluids that essentially bring to an increase in radiogenic Pb (about 19.0 $^{206}Pb/^{204}Pb$) and to values of 0.710 $^{87}Sr/^{86}Sr$ and of $-10‰$ $\delta^{11}B$. The recognition of different stages of interaction between mantle rocks and sedimentary/crustal reservoirs allows us to define the geochemical effects related to the early coupling of such rocks along the plate-interface. Our study shows that ultramafic rocks involved in subduction-zone metamorphism and serpentinization uptake radiogenic Pb and Sr released by associated sedimentary reservoirs. The exchange process envisioned here is not only representative of subduction mélanges: it can also be a proxy of mass transfer between slab and serpentinized supra-subduction mantle, as occurs in forearcs. Dehydration of the Gagnone-type serpentinized mantle releases crust-derived components to arcs, without direct involvement of metasediment dehydration and/or melting in subarc environments. The retention of appreciable amounts of fluid-mobile elements, radiogenic Pb and Sr in dehydrated Gagnone peridotites has implications on element recycling in the deep Earth's mantle.

* Corresponding author.
E-mail address: enrico.cannao@unige.it (E. Cannaò).

http://dx.doi.org/10.1016/j.gca.2015.04.024
0016-7037/

1. INTRODUCTION

Increasing evidence suggests that the interface between converging plates consists of hydrated low-viscosity layers that are relevant to mantle re-fertilization, arc magmatism, subduction and exhumation tectonics (Bebout, 2014). Plate-interface settings are sites of tectonic accretion of slab- and mantle-derived materials and of strong fluid and deformation channeling. These features favour geochemical exchange between different rock systems in subduction zones and affect slab-to-mantle mass transfer and arc magmatism (e.g. Bebout and Barton, 2002; Bebout, 2007; Marschall and Schumacker, 2012; Spandler and Pirard, 2013; Angiboust et al., 2014). Geophysical data and modelling studies suggest persistence of such layers atop of subducting plates down to sub arc depths (Bostock et al., 2002; Gerya et al., 2002; Syracuse et al., 2010; Friederich et al., 2014).

Plate-interface domains may either consist of altered mantle wedge, or of mélanges showing mixing and hybridization of various lithologies. In the first case, km-thick layers of serpentinite formed in the supra-subduction mantle by uprising slab fluids allow storage of fluid-mobile trace elements (Peacock, 1993; Hyndman and Peacock, 2003; Savov et al., 2005, 2007; Scambelluri and Tonarini, 2012; Deschamps et al., 2013). The capacity of serpentinized mantle rocks to incorporate volatiles, fluid-mobile elements, halogen- and noble gas, makes them a candidate, together with metasediments, as element carriers down to sub arc depths (e.g. Benton et al., 2001; Scambelluri et al., 2001, 2004, 2014; Deschamps et al., 2011; John et al., 2011; Kendrick et al., 2011; Kodolányi et al., 2012; Debret et al., 2013; Lafay et al., 2013). In case of mélanges, serpentinite, metasediments (from subducted accretionary and trench complexes) and locally mafic components are dominant matrix lithologies in which slices of slab and overlying mantle become tectonically embedded (Bebout et al., 1999; Bebout and Barton, 2002; Breeding et al., 2004; King et al., 2006, 2007; Marschall et al., 2006; Malatesta et al., 2012). Serpentinized mantle wedge and plate interface mélanges are now considered the carriers of water and of a large spectrum of fluid-mobile elements.

The fluid-mobile element boron and its isotopes are efficient tracers of fluid-mediated mass transfer in subduction settings, enabling to define a link between subduction input and arc output (e.g. Moran et al., 1992; Bebout et al., 1993; Ryan and Langmuir, 1993; Leeman, 1996; Peacock and Hervig, 1999; Tonarini et al., 2001, 2007, 2011; Rosner et al., 2003; Marschall and Schumacker, 2012; Scambelluri et al., 2014). Boron, coupled with Sr and Pb isotopic systems, is a useful tracer of the exchange between crust- and mantle-derived lithologies in plate interface settings (e.g. King et al., 2006, 2007). Applying the above isotopic systems to high-pressure mélanges can improve our understanding of interaction between different subducting reservoirs and the composition of fluids released by dehydrating mélange lithologies.

In this work we focus on fluid-mobile element exchange between ultramafic–mafic blocks and metasediments in the subduction mélange of Cima di Gagnone (Adula-Cima Lunga nappe, Central Alps; Evans and Trommsdorff, 1978, Evans et al., 1979). High concentrations of B, Be, As, Sb, Pb in the Gagnone peridotite suggest interactions with sedimentary reservoirs during subduction (Scambelluri et al., 2014). Here we present the B, Sr and Pb isotopic compositions of ultramafic, mafic and metasedimentary rocks from Gagnone to discuss: (I) the exchange processes between the different rock reservoirs; (II) the timing of isotopic exchange (wether prograde, peak, or retrograde); (III) the tectonic coupling among mélange-forming lithologies and (IV) the possible implications with arc magmatism.

2. GEOLOGICAL SETTING

The Adula-Cima Lunga Unit (Central Alps) belongs to the southernmost European margin involved in Alpine subduction (Schmid et al., 1996, 2004). It consists of orthogneiss and metasediment hosting mafic–ultramafic bodies recording eclogite-facies metamorphism at pressure–temperature conditions increasing from north (1.2 GPa – 500 °C) to south (2.5 GPa – 850 °C) (Evans and Trommsdorff, 1978; Heinrich, 1978, 1982, 1986; Evans et al., 1979; Meyre et al., 1997, 1999). In southern Adula, kilometre- to metre-sized bodies of high-pressure peridotite (Alpe Arami, Monte Duria, Cima di Gagnone) are embedded in crustal rocks (Fig. 1; Mockel, 1969; Fumasoli, 1974; Evans and Trommsdorff, 1978; Heinrich, 1982; Pfiffner and Trommsdorff, 1998; Trommsdorff et al., 2000). In Cima di Gagnone, eclogite-facies crystallization of garnet peridotite and of associated chlorite harzburgite occurred at 2.5–3.0 GPa and 750–800 °C (Nimis and Trommsdorff, 2001; Scambelluri et al., 2014). The ultramafic rocks contain layers of eclogite and metarodingite, representing primary basaltic/gabbroic intrusions with MORB type geochemical affinity (Evans et al., 1979, 1981; Pfiffner, 1999). Presence of eclogites confirms that the Gagnone rock-suite underwent subduction zone metamorphism: the rodingite indicates that ultramafic rocks were serpentinized prior to peak eclogite facies recrystallization (Evans and Trommsdorff, 1978). The Gagnone metaperidotites thus represent dehydration products of serpentinized mantle recording full antigorite-breakdown (Evans and Trommsdorff, 1978). Their enrichment in fluid-mobile B, As, Sb, U and Th, compared to abyssal serpentinites (Kodolányi et al., 2012; Deschamps et al., 2013) points to multiple hydration events: an early-stage oceanic serpentinization followed by interaction with metasedimentary reservoirs during subduction burial, once peridotites were embedded inside host metasediments (Scambelluri et al., 2014).

The Adula metasedimentary rocks mainly correspond to gneiss and metapelite with minor amounts of Mesozoic dolomite and quartzite (Fig. 1). The high-pressure paragenesis consists of garnet, paragonite, phengite + kyanite + quartz + omphacite (Heinrich, 1982). An Oligocene–Miocene amphibolite-facies overprint is widespread in the Adula unit and often fully overprints the high-pressure event (Trommsdorff, 1966; Heinrich, 1982, 1986; Grond et al., 1995; Stampfli et al., 1998; Negel

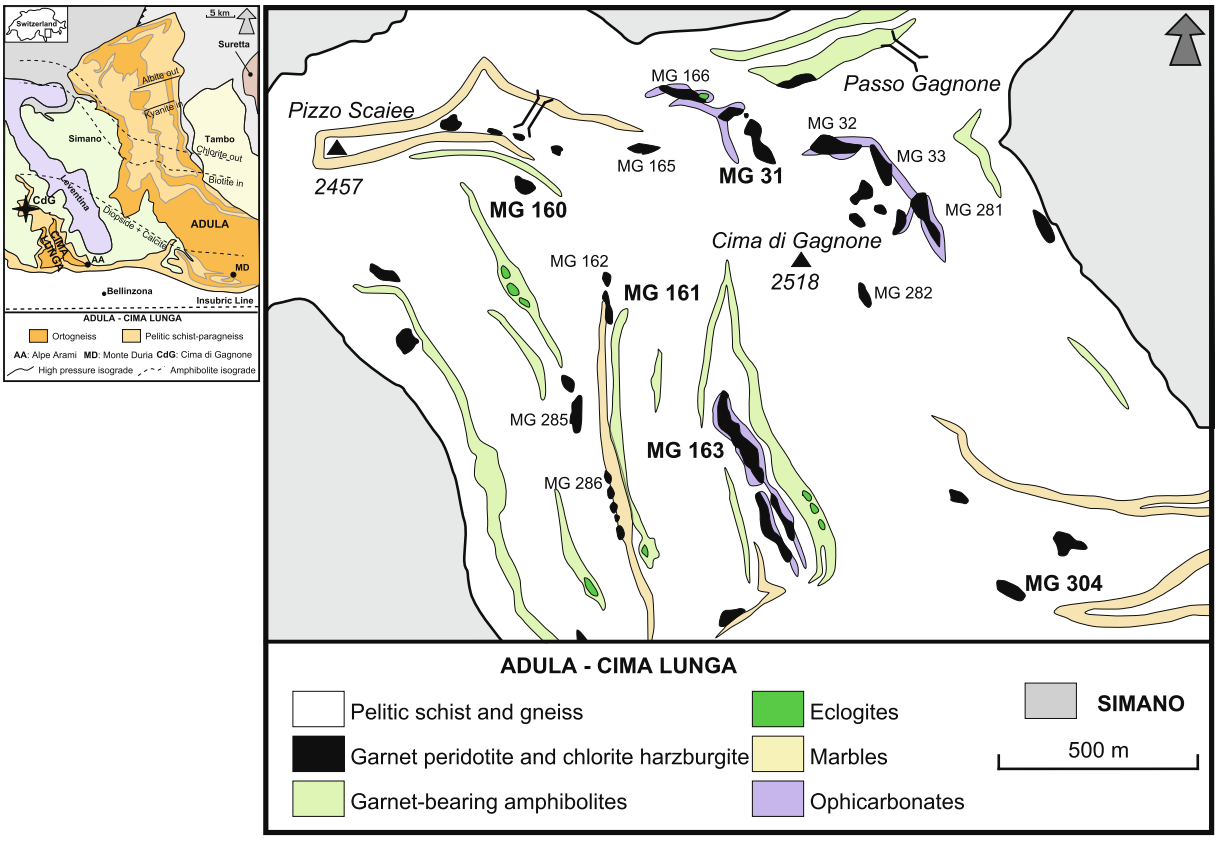

Fig. 1. Geological map of the Cima di Gagnone area showing the main outcrop of ultramafic rock bodies (MG XXX, as mentioned in previously works). Labels with large font size indicate the garnet peridotite and chlorite harzburgite suite rocks isotopically analysed in this study. Redrawn and modified after Pfiffner and Tromsdorff (1998) and Pfiffner (1999).

et al., 2002). Retrograde products are (i) phengite recrystallization in gneiss and paraschists, (ii) amphibolitic symplectites after omphacite and garnet and of garnet + hornblende-bearing assemblages at the expense of the eclogite minerals, and (iii) amphibolite-chlorite-blackwalls around metarodingite (Evans et al., 1979; Heinrich, 1982). Pressure–temperature conditions for amphibolite-facies retrogression are 6–7 kbar and 600–650 °C (Heinrich, 1982).

Eclogite-facies Sm-Nd and Lu-Hf ages of 40 Ma have been obtained on garnet-clinopyroxene-whole-rock in garnet peridotites (Becker, 1993; Brouwer et al., 2005). 43–45 Ma were determined using in U-Pb zircon dating (Gebauer et al., 1992; Gebauer, 1996). Such dates are consistent with the age of peak high-pressure subduction metamorphism in the Western Alps (Berger and Bousquet, 2007). The rock association of Adula Cima-Lunga unit has long been interpreted as a lithospheric mélange (Trommsdorff, 1990) formed in a tectonic accretionary channel (Engi et al., 2001), a view recently supported by the geochemical study of peridotites (Scambelluri et al., 2014). This hypothesis is contrasted by the discovery of Varisican Lu-Hf ages (332.7 Myr) in an eclogite from Trescolmen, that enabled Herwartz et al. (2011) to recognize two orogenic cycles in Adula and to propose that Adula behaved as a coherent unit during Alpine subduction.

3. SAMPLES PETROGRAPHY AND MICROSTRUCTURE

3.1. Ultramafic rocks

Ultramafic rocks from this area correspond to garnet peridotite, chlorite harzburgite and dunite. Detailed description of the garnet peridotite and of several chlorite harzburgite samples analyzed here are provided by Scambelluri et al. (2014). Here we briefly present such samples, and we provide more detailed description of new chlorite harzburgite (MG31 09-06; MG163 09-07) and dunite (MG163 12-03) samples.

The garnet peridotite samples (MG160 09-10; MG160 96-2; MG160 4/8; MG161 92-1) show an eclogitic foliation with olivine, orthopyroxene, clinopyroxene, garnet and Mg-hornblende. Ilmenite intergrown with olivine replaces former Ti-clinohumite. Poikiloblastic garnet encloses pre-eclogitic orthopyroxene, chlorite, Ca-amphibole and spinel inclusions (Scambelluri et al., 2014).

The foliated chlorite harzburgite samples MG31 09-06 and MG163 09-07 are similar to samples MG31 09-01, MG163 09-05 of Scambelluri et al. (2014). These rocks show an olivine, orthopyroxene and chlorite foliation that, in the field, is parallel to the high-pressure foliation of eclogite and metarodingite. Accessory phases are

magnetite, ilmenite and Fe-rich chromite. Sulfides are associated with chromite both as inclusions inside silicate minerals and as tiny interstitial grains. The underformed chlorite harzburgite samples MG304 92-1 and MG304 92-2 show coarse-grained, randomly-oriented, idiomorphic orthopyroxene, olivine and interstitial chlorite, associated with minor modal amounts of magnetite, diopside and F-bearing Ti-clinohumite (Scambelluri et al., 2014). Serpentine inclusions in clinohumite from these rocks demonstrate harzburgite derivation from serpentinized protoliths (Scambelluri et al., 2014).

The dunite sample MG163 12-03 is characterized by olivine and chlorite disposed along a main foliation. Magnetite, ilmenite and chromite are the accessory minerals.

Retrograde tremolite, cummingtonite and talc with random-orientation overgrow the high-pressure minerals in all peridotites.

3.2. Eclogite, metarodingite and retrograde equivalents

Samples were collected in outcrops MG31 and MG163 (Figs. 1 and 2). Eclogite MG163 12-10 consists of equigranular omphacite, garnet and quartz, with minor ilmenite, rutile, epidote and amphibole. Omphacite is overgrown by plagioclase, diopside and amphibole symplectites (Fig. 3A). Coarse idiomorphic garnet (1–3 mm sized) hosts quartz, plagioclase, amphibole and clinopyroxene inclusions. Garnet is often surrounded by green hornblende (Fig. 3A). Sample MG163 12-11 is a retrogressed domain of MG163 12-10, collected in outcrop MG163 along the rim of an eclogitized mafic dike (Fig. 2A). Omphacite here is replaced by hornblende at the core and by plagioclase and hornblende symplectite at the rim. Garnet is overgrown by the same symplectite present in clinopyroxene rims. Retrograde amphibolite-facies metamorphism leading to formation of garnet-bearing or garnet-free amphibolite is common to the entire Adula Unit.

Metarodingite (MG31 12-07, Figs. 2 and 3B) displays two generations of garnet: old and coarse-grained garnet (garnet 1) occurs in relict crystals replaced by younger, fine-grained and homogeneous garnet 2. Diopside is in textural equilibrium with garnet 2 in the high-pressure paragenesis. Epidote, titanite and rutile are accessory phases. At the contact with the surrounding ultramafic rocks rodingite

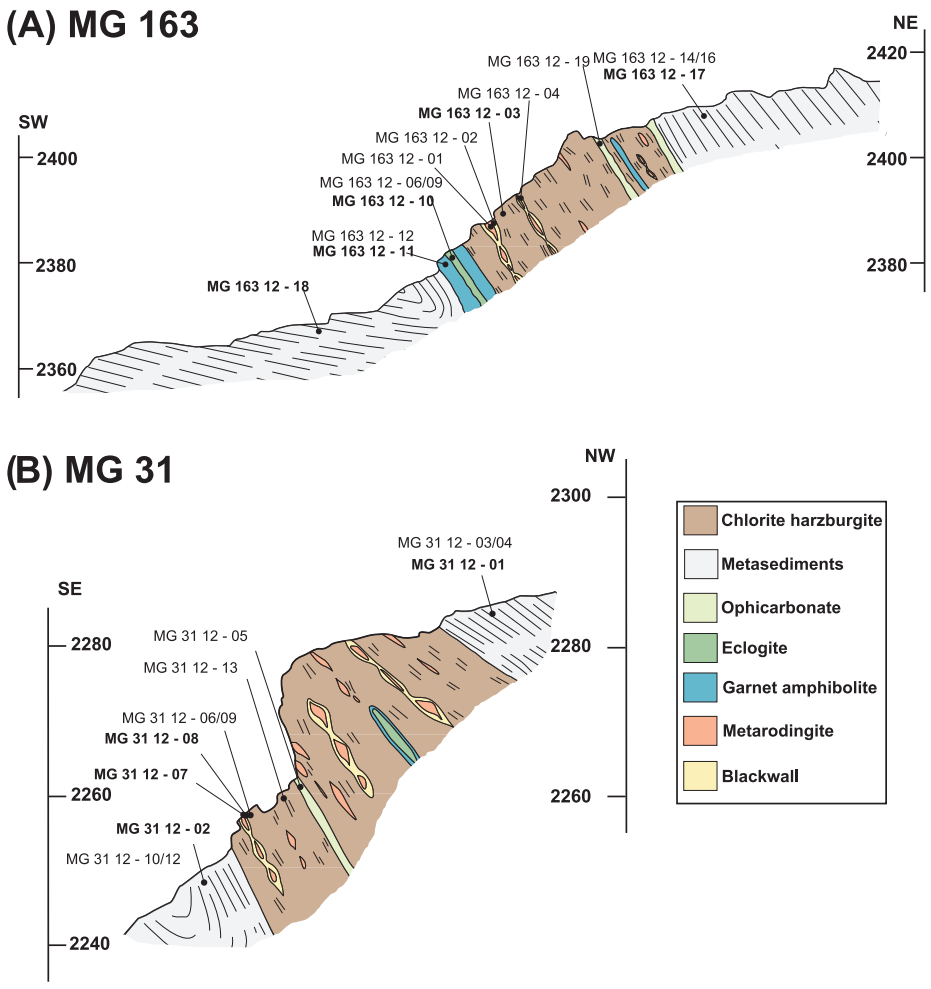

Fig. 2. Interpretative geological section with location of the samples for the main two chlorite harzburgite outcrop MG 163 (A) and MG 31 (B) (redrawn after Pfiffner, 1999). Bold labels refer to samples analyzed in this work.

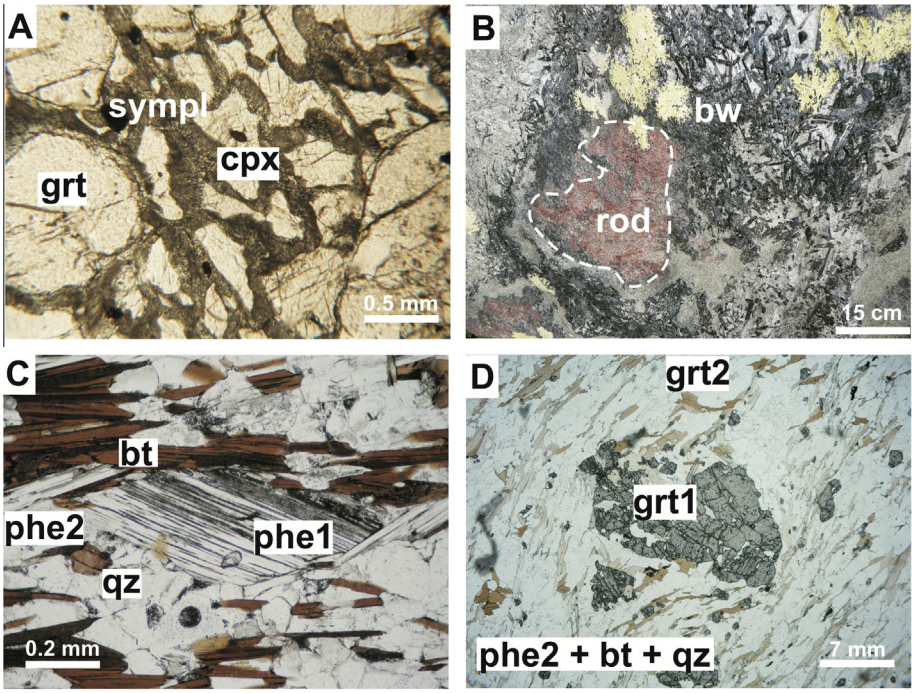

Fig. 3. Micro- and field-photographs of the main lithologies. (A) Eclogite sample (MG163 12-10) showing weakened foliation of clinopyroxene (cpx) and garnet (grt). Along the grain boundaries are present evidence of partial retrogression by symplectite (sympl) made of amphibole, plagioclase and orthopyroxene: rock-forming minerals of the retrograde amphibolite MG163 12-11. (B) Core of metarodingite (rod, MG31 12-07) surrounding by retrograde amphibolitic blackwall (bw, MG31 12-08). (C) Mica-fish microstructure in gneiss (MG163 12-17) suggesting an ancient stage of high pressure event recorded in the country rocks (phe1: high pressure phengite with Si = 3.36 a.p.f.u. and XCel = 0.24). The main foliation is made of phengite (phe2 Si = 3.22 a.p.f.u. and XCel = 0.14), garnet, biotite (bt), quartz (qz) and plagioclase. (D) Rotated pseudoblast of high pressure garnet (grt1) recrystallized in amphibolite conditions. Retrograde paragenesis is made of phengite (phe2), garnet (grt2), biotite (bt), quartz (qz) and plagioclase.

displays retrograde blackwalls (MG31 12-08, Fig. 3B) composed of amphibolite-facies hornblende + epidote overgrowing the previous high-pressure metarodingite minerals.

3.3. Country gneiss and micaschist

The sampled gneiss (MG31 12-01; MG31 12-02; MG163 12-17; MG163 12-18; Fig. 2) and micaschist (MG160 12-04) show a main foliation with syn-tectonic minerals locally overgrown by static post-kinematic crystals. Phengite and garnet relics (phe1, grt1) predating foliation development are less common (MG163, MG31 gneiss; Fig. 3C and D). The gneiss from outcrop MG31 contains biotite, quartz and plagioclase with variable modal garnet and white mica. It also shows relatively high abundance of high-pressure mica relics. In samples MG31 12-01 and MG31 12-02 quartz and plagioclase occur as slightly elongated equigranular grains and biotite forms a well defined foliation. MG31 12-01 also shows a weak secondary schistosity formed by a new generation of biotite 2 and chlorite cutting the previous foliation. Two size distributions of garnet are observed: larger (1–4 mm in diameter, Fig. 3D) with numerous inclusions of fine-grained mica and quartz, and small grains (up to 0.5 mm in diameter).

Samples from outcrop MG163 are quite similar to gneiss MG31 in terms of mineralogy and texture. The MG163 samples display higher contents in white mica either coexisting with biotite parallel to the foliation, or forming relics in earlier high-pressure mica-fish microstructures (phe1, Fig. 3C). Accessory minerals in MG163 gneiss are zircon, apatite, rutile, ilmenite and clinozoisite.

Micashist MG160 12-04 shows a main foliation made of white mica anastomosing around microlithons consisting of relict mica flakes. Coarse and rotated grains of inclusion-free garnet with irregular boundaries are present and sometimes are replaced by biotite and quartz. Biotite overgrows white mica and garnet. Minor REE-rich epidote occurs parallel to the schistosity.

4. METHODS

4.1. ICP-MS

Bulk trace element concentrations were determined by inductively coupled plasma–mass spectrometry (ICP-MS) at Géosciences Montpellier (University of Montpellier, France) using an Agilent 7700× quadrupole ICP-MS, following the procedure described in Ionov et al. (1992) and in Godard et al. (2000). 100 mg aliquots of samples were dissolved in a HF/HClO4 mixture in screw-top Teflon beakers then diluted by a factor of 1000, 2000 and 4000 for ultramafic, mafic and sialic rocks, respectively. In and Bi were used as internal standards during ICP-MS measurements. We used external calibration solution using

multi-element standard solution (Merck) except for Nb and Ta. To avoid memory effects due to the introduction of concentrations Nb-Ta solutions in the instrument, Nb and Ta concentrations were determined by using, respectively, Zr and Hf as internal standards. This surrogate calibration technique is adapted from the method described by Jochum et al. (1990) for the determination of Nb by spark-source mass spectrometry. The Helium cell gas mode of the Agilent 7700× was used to measure Sc, V, Mn, Co, Ni, Cu, Zn and As, while removing polyatomic interferences. We used as standards BHVO_1, BEN and OU_6 for trace-element rich rocks, like gneiss, micaschist and blackwall, UBN, BIR_1 and MRG_1 for intermediate mafic rocks and JP_1 and DTS1 for depleted chlorite harzburgite. Detailed description of the method and detection limits can be found in Godard et al. (2000).

4.2. TIMS

Boron concentrations were determined by isotope dilution using the NIST SRM 982 spike. B concentration in isotope dilution and boron isotopic composition were determined using a single collector VG Isomass 54E positive thermal ionization mass spectrometer running in dynamic mode at IGG-CNR of Pisa (Italy). Boron was extracted through alkaline fusion and purification by ion-exchange procedure (Tonarini et al., 1997). Estimated reproducibility for B concentration is about 2.5% (Tonarini et al., 2003), whereas the accuracy of B isotope composition, evaluated by repeated analyses of the NIST SRM 951 standard taken through the full chemistry, is about ±0.5‰. Boron isotopic compositions of the samples are reported in the conventional delta notation ($\delta^{11}B$) as permil (‰) deviation from accepted composition of NIST SRM 951 (certified $^{11}B/^{10}B = 4.04362$; Catanzaro et al., 1970).

Sr isotope analyses were performed using a Finnigan MAT 262 multicollector mass-spectrometer (at IGG-CNR, Pisa) running in dynamic mode, after ion-exchange purification through Sr-spec resin. Measured $^{87}Sr/^{86}Sr$ ratios have been normalized to $^{86}Sr/^{88}Sr = 0.1194$. Replicate analyses of NIST SRM 987 ($SrCO_3$) standard gave an average value of 0.710207 ± 13 (2SD, $n = 47$). Published values are adjusted to $^{87}Sr/^{86}Sr = 0.710250$. Sr blanks were about 0.3 ng, which are negligible for the analyzed samples.

Pb isotope analyses were performed using a Finnigan MAT 262 multicollector mass-spectrometer at IGG-CNR of Pisa (Italy), operating in static mode, with conventional extraction by chromatographic ion exchange in Dowex 1 anion resin, using standard HBr and HCl elution procedures. Replicate analyses of Pb isotope ratios are accurate to within 0.025% (2SD) per mass unit, after applying mass discrimination corrections of $0.15 \pm 0.01\%$ per mass unit relative to the NIST SRM 981 reference composition of Todt et al. (1993). Pb blanks were on the order of 0.2–0.4 ng during the period of chemistry processing, and no blank correction was made.

Sr and Pb data are reported with age correction using, respectively, the concentration of Rb, Sr and of U, Th and Pb from ICP-MS analyses. For eclogite metamorphic rocks we use an age of 40 Ma (Becker, 1993; Brouwer et al., 2005) and an age of 35 Ma for amphibolite retrograde event (Gebauer et al., 1992).

5. RESULTS

5.1. Bulk rock major, rare earth and trace element composition

Bulk-rock major and trace element contents were determined in the Gagnone chlorite harzburgite and dunite (MG31 09-06; MG163 09-07; MG163 12-03), in eclogite, metarodingite and their retrograde equivalents (MG163-12-10; MG163 12-11; MG31 12-07; MG31 12-08), and in host paragneiss and micaschist (MG31 12-01; MG31 12-02; MG163 12-17; MG163 12-18; MG160 12-04; see Appendix Table A-1). Data on the Gagnone garnet peridotite and chlorite harzburgite from Scambelluri et al. (2014) are also reported for comparison. In Fig. 4[1], the color filled symbols refer to the ultramafic rocks analysed here for major, trace elements and isotopes (also filled grey symbols) whereas open grey symbols refer to samples analysed in previous works (Scambelluri et al., 2014). Since the Alpine high-pressure Erro-Tobbio serpentinized peridotite has been defined here as the potential protolith of Gagnone, Table A1 also reports new trace element analyses of selected Erro-Tobbio samples.

5.2. Ultramafic rocks – chlorite harzburgite

5.2.1. Major elements

Our LOI values for the Gagnone chlorite harzburgite and dunite range between 1.33 and 3.77 wt% and are comparable with the 0.13–5.66 wt% range by Scambelluri et al. (2014) for the same rock-type. Overall, the whole Gagnone peridotite sample set analyzed here and by Scambelluri et al. (2014) shows negative linear correlations of MgO vs CaO, Al_2O_3 and SiO_2: some chlorite harzburgite has very low CaO (below detection limit) and 1.03 wt% Al_2O_3 (Table A1). These low concentrations could reflect variable intensity of serpentinization, which caused loss of these elements due to clinopyroxene replacement. The Mg values are rather constant for garnet peridotite (Mg# = 0.82–0.84; Scambelluri et al., 2014) whereas are more variable for chlorite harzburgite (Mg# up to 88).

5.2.2. Rare earth elements

The REE compositions of the Gagnone chlorite harzburgite and dunite are reported in Fig. 4A. All samples analyzed here and in previous works (Scambelluri et al., 2014) show REE concentrations lower than those in primitive mantle (PM; McDonough and Sun, 1995). The chlorite harzburgite MG31 09-06 shows flat HREE to MREE patterns with moderate depletion in LREE. Sample MG163 09-07 shows depletion from HREE to MREE

[1] For interpretation of color in Fig. 4, the reader is referred to the web version of this article.

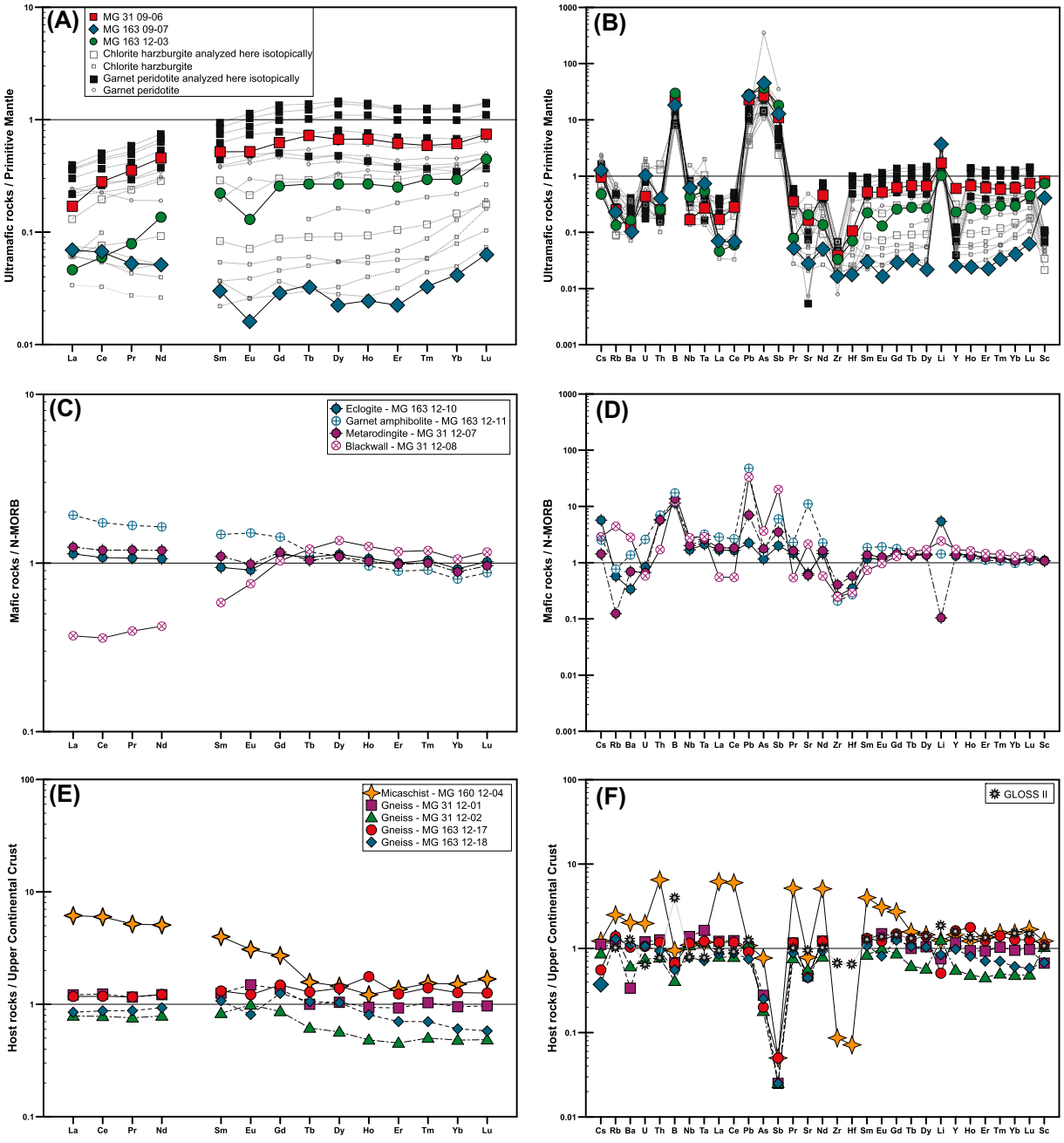

Fig. 4. (A) and (B) Primitive mantle normalized bulk-rocks REE and trace elements patterns of the chlorite harzburgite and dunite rocks (from McDonough and Sun, 1995). For comparison are reported others chlorite harzburgite and garnet peridotites from Gagnone (data from Scambelluri et al., 2014). (C) and (D) N-MORB normalized bulk-rocks REE and trace elements patterns of high pressure and retrograde equivalent mafic rocks (Onishi and Sandell (1955); Sun and McDonough (1989) for As value; Jochum and Hofmann (1997) for Sb value). (E) and (F) Upper continental crust (UCC) normalized bulk-rocks REE and trace elements patterns of the host rocks (Rudnick and Gao, 2003). In the spider diagram are also reported the GLOSSII for comparison (Plank, 2014).

and enrichment in LREE relative to MREE, like a spoon-shape pattern with a negative Eu anomaly. This sample has the lowest concentration of HREE of all the samples analysed in this study. The dunite sample MG163 12-03 displays the same pattern of previously analyzed rocks and is characterized by slight REE depletion and by negative Eu anomaly.

5.2.3. Trace elements

All samples show positive anomalies in the fluid-mobile elements B, Pb, As, Sb and Li, a feature common to all ultramafic rocks from Gagnone (Fig. 4B, see also Scambelluri et al., 2014). Though comparable with results of Scambelluri et al. (2014), our samples present higher values in Sc and lower U contents.

5.3. Mafic rocks – eclogite, metarodingite and their retrograde equivalents

5.3.1. Major elements

The bulk-rock major element contents of eclogite and metarodingite presented here are quite similar to those presented in previous works (Evans et al., 1981; Pfiffner, 1999). Eclogite has CaO, Na_2O and K_2O concentrations (10.87, 2.82 and 0.01 wt%, respectively) compatible with values of igneous mafic rocks. Compared with eclogite, metarodingite has higher CaO (20.23 wt%) and much lower alkali and SiO_2 contents (0.05 wt% Na_2O; 44.29 wt% SiO_2) that reflect the rodingitization process. The protolith of these mafic rocks was identified as a tholeiitic basalt on the basis of TiO_2, HREE and other immobile trace elements, like Zr and Hf (Evans et al., 1979, 1981). Retrograde metamorphism produced significant variations in the major element values in garnet amphibolite after eclogite and in the amphibole blackwall after metarodingite. Both lithologies record loss in SiO_2 (49.1–45.8 wt%), Fe_2O_3 (13.4–12.6 wt%), Na_2O (2.8–0.74 wt%) and TiO_2 (1.8–1.6 wt%). In the garnet amphibolite MG163 12-11 decreases in the above elements is accompanied by increases in Al_2O_3 (12.8–15.6 wt%), MgO (8.9–10.6 wt%), CaO (10.8–12.3 wt%), K_2O and H_2O (expressed by LOI value) and quite invariate MnO and P_2O_5. With respect to metarodingite, the blackwall has higher Al_2O_3 (11–14 wt%), MnO (0.18–0.28 wt%), MgO (9.0–13.5 wt%), Na_2O (0.05–1.5 wt%), K_2O and P_2O_5 (0.2–0.55 wt%) associated with a lost of SiO_2 (44.3–40.9 wt%), Fe_2O_3 (12.3–12.1 wt%), CaO (20.2–13.9 wt%) and TiO_2 (1.9–1.4 wt%).

5.3.2. Rare earth elements

Eclogite and metarodingite show flat REE patterns at about 1, normalized to N-MORB values (Fig. 4C, Sun and McDonough, 1989), with slight enrichment in LREE. In contrast, their retrograde products show quite different and somehow inverted patterns. The garnet amphibolite MG163 12-11 shows HREE to MREE patterns analogous to the eclogite protolith and displays LREE enrichment up to 2 times the reference N-MORB, with $La_N/Nd_N = 1.30$ and $La_N/Lu_N = 2.67$. The blackwall sample MG31 12-08 is strongly LREE-depleted and slightly HREE-enriched with respect to the metarodingite protolith. This amphibole-rich reaction zone inherits a garnet like pattern, with $La_N/Nd_N = 0.64$ and $La_N/Lu_N = 0.38$.

5.3.3. Trace elements

The eclogite sample MG163 12-10 and the metarodingite MG31 12-07 show quite similar trace elements spidergrams (Fig. 4D), with absolute trace element contents higher than N-MORB values (Onishi and Sandell, 1955, for As value; Sun and McDonough, 1989; Jochum and Hofmann, 1997, for Sb value) with the exception of Ba, U, Cs and Li for the metarodingite. In particular, positive anomalies in B, As, Sb and negative anomalies in Sr, Zr, Hf are visible in both rocks; moreover, a Li negative anomaly pertains to the eclogite. The garnet amphibolite MG163 12-11 is enriched in fluid mobile elements, in particular in Ba, U, As, Sb and Sr with respect to the eclogite protolith. Compared to metarodingite, the blackwall sample MG31 12-08 is enriched in Rb, Ba, As, Sb, Pr, Sr and Li. The enrichment in LREE and fluid mobile elements in the retrograde garnet amphibolite with respect to eclogite protolith can reflect the change in mineralogy.

5.4. Host rocks – gneiss and micaschist

5.4.1. Major elements

The country paragneiss contains high SiO_2 concentrations (66.28–71.17 wt%), up to 14.65 wt% Al_2O_3 and about 6 wt% Fe_2O_3. Other major elements like MgO, CaO, Na_2O, K_2O are present in few wt% or less than 1 wt% (MnO, TiO_2 and P_2O_5). Water is present with a maximum value of 1.51 wt% in sample MG 163 12-18. Compared with paragneiss, the micaschist MG160 12-04 has lower SiO_2 (48.26 wt%), Na_2O (1.90 wt%) and P_2O_5 (0.01 wt%) and has higher Al_2O_3 (25.11 wt%), MgO (5.22 wt%), K_2O (7.06 wt%) and TiO_2 (1.20 wt%). Other major elements are comparable with those of the gneiss. In the micaschist, the water content is 2.46 wt%, i.e. higher than all analyzed country rock samples.

5.4.2. Rare earth elements

The rare earth element compositions of the felsic country rocks normalized to the upper continental crust (UCC, Rudnick and Gao, 2003) are reported in Fig. 4E. The flat REE pattern of paragneiss MG31 12-01 ranges around 1 UCC: it is characterized by a small Eu anomaly and is different from the REE pattern of sample MG31 12-02, showing MREE to HREE depletion below 1 UCC. The duality in REE patterns discussed above is also common to the paragneiss samples from outcrop MG163. Sample MG163 12-17 has a flat pattern and absolute REE contents slightly above 1 UCC. Differently, sample MG163 12-18 has normalized HREE contents below the UCC. The highest REE contents are shown by the micaschist MG160 12-04, which displays flat HREE to MREE patterns and a significant enrichment in MREE to LREE up to 6 times the UCC ($La_N/Lu_N = 3.65$).

5.4.3. Trace elements

The trace element compositions of the country Gneiss and Micaschist host rocks are shown in Fig. 4F. The gneissic samples from outcrops MG31 and MG163 display similar patterns; the absolute amounts of normalized LILE, LREE, MREE range around the UCC and are grossly comparable with the Global Subducted Sediment reservoirs (GLOSS II, Plank, 2014). As outlined above and in Fig. 4F, exception is done for the HREE depletion shown by MG31 12-02 and MG163 12-18. Different from the gneiss samples, micaschist MG160 12-04 has much higher contents in MREE, LREE, Th and, to a minor extent, of Rb, Ba, U. Negative anomalies in B, As, Sb, Sr, Zr, Hf (the last two only for the micaschist) are common to all country rock samples analysed. Ba contents below the UCC and GLOSS II only pertain to samples MG31 12-02 and MG31 12-01.

5.5. Bulk-rock isotopic compositions

The isotopic data produced for the Cima di Gagnone rock-suite are shown in Table 1. Previously published bulk B contents, B- and Sr-isotope data of the Erro-Tobbio serpentinites (Scambelluri and Tonarini, 2012), are also reported in Table 1 together with new Pb isotope data for comparison and discussion (see Section 6).

The Rb, Sr and the U, Th, Pb concentrations obtained with the ICP-MS technique were used for the age correction of the Sr and Pb isotopic values, respectively. For this correction, we adopted the metamorphic age of 40 My for the eclogitic peak (Becker, 1993; Brouwer et al., 2005) and of 35 My for the amphibolite retrograde event (Gebauer et al., 1992). Assuming that the average concentrations of Pb, U, Th, Rb, Sr in the Erro-Tobbio serpentinized mantle peridotites (Table A1) represent the starting values of the Gagnone metaperidotite protolith, the difference in the Pb and Sr isotopic composition of Gagnone achieved using an eclogitic (40 My) or a Jurassic oceanic (160 My) age correction is negligible. This is due to the high Pb/U, Pb/Th, Sr/Rb ratios of Erro-Tobbio samples (Table 1). Therefore, here we adopt an age corrections to 40 My for the best preserved eclogite-facies rocks and to 35 My for the retrogressed samples.

5.5.1. Ultramafic rocks

All ultramafic rocks samples show negative $\delta^{11}B$ values (Table 1; Fig. 5A). The garnet peridotite has values ranging between −3‰ to −9‰; the chlorite harzburgite plus dunite show comparable values, from −5‰ to about −9‰. The Sr isotopic compositions are higher than the depleted mantle and the Jurassic seawater values. For the garnet peridotite, $^{87}Sr/^{86}Sr$ values range from 0.71119 to 0.71244 (Fig. 5B) whereas the chlorite harzburgite shows less radiogenic $^{87}Sr/^{86}Sr$ values from 0.70896 up to 0.71087. The garnet peridotite has Pb isotope compositions much higher than the depleted mantle (Fig. 5C) and displays $^{206}Pb/^{204}Pb$ ratios from 18.549 to 18.716, $^{207}Pb/^{204}Pb$ from 15.644 to 15.751, and $^{208}Pb/^{204}Pb$ from 38.758 to 39.125. Chlorite harzburgite and dunite have more scattered values relative to the other ultramafic rocks, and range from 18.292 to 18.837 for $^{206}Pb/^{204}Pb$, from 15.617 to 15.667 for $^{207}Pb/^{204}Pb$ and from 38.170 to 38.604 for $^{208}Pb/^{204}Pb$. Fig. 5C just reports the $^{206}Pb/^{204}Pb$ ratio because it appears more sensitive of the fluid-rock interactions recorded by the Gagnone rocks. We report the Pb/Pb isotopic diagrams showing variations in $^{207}Pb/^{204}Pb$ and $^{208}Pb/^{204}Pb$ in the Electronic Appendix. These diagrams show that the Gagnone ultramafic and mafic rocks grossly plot in-between the Gagnone paragneiss and the hypothesized Erro-Tobbio protoliths, and essentially confirm what shown in Fig. 5C (see Electronic Appendix).

5.5.2. Eclogite – metarodingite mafic rocks and retrograde association

High-pressure mafic rocks have $\delta^{11}B$ values of –1‰ and −6‰ for eclogite and metarodingite, respectively. The eclogite has a radiogenic Sr isotope value of 0.70844, higher than the primitive mantle and Jurassic seawater ($^{87}Sr/^{86}Sr = 0.7070$). The metarodingite shows slightly lower value of 0.70730 of $^{87}Sr/^{86}Sr$ ratio. Pb isotope values for these mafic rocks are higher than the primitive mantle and MORB values ($^{206}Pb/^{204}Pb = 18.519$, $^{207}Pb/^{204}Pb = 15.660$, $^{208}Pb/^{204}Pb = 38.563$ for eclogite and $^{206}Pb/^{204}Pb = 18.553$, $^{207}Pb/^{204}Pb = 15.652$ and $^{208}Pb/^{204}Pb = 38.510$ for metarodingite). Compared to eclogite and metarodingite, the retrograde garnet amphibolite and blackwalls display lower $\delta^{11}B$ (Table 1) and higher Sr and Pb isotope ratios (Fig. 5B and C). Garnet amphibolite has $\delta^{11}B$ of −5‰, $^{87}Sr/^{86}Sr$ 0.70954, $^{206}Pb/^{204}Pb$ of 18.788, $^{207}Pb/^{204}Pb$ of 15.678 and $^{208}Pb/^{204}Pb$ of 38.824; blackwalls on metarodingite have $\delta^{11}B$ of −8‰, $^{87}Sr/^{86}Sr$ 0.70789, $^{206}Pb/^{204}Pb$ of 18.940, $^{207}Pb/^{204}Pb$ of 15.690 and $^{208}Pb/^{204}Pb$ of 38.788.

5.5.3. Metasediments

Gneiss and Micaschist have negative $\delta^{11}B$ ranging from −3‰ to −12‰ (Table 1, Fig. 5A). These values correspond with other values of metasedimentary rocks described in literature (e.g. from −5‰ to −17 ‰ in Ishikawa and Nakamura, 1994; or from −7‰ to −15‰ in Bebout and Nakamura, 2003). The $^{87}Sr/^{86}Sr$ ranges between 0.71124 and 0.72866, and the $^{206}Pb/^{204}Pb$ ranges between 18.743 and 18.978. The $^{206}Pb/^{204}Pb$ values negatively correlate with $^{87}Sr/^{86}Sr$ (Table 1, Fig. 5B). The $^{207}Pb/^{204}Pb$ and $^{208}Pb/^{204}Pb$ ratios range between 15.658–15.681 and 38.673–39.240, respectively (Table 1, Fig. 5C).

6. DISCUSSION

In the last decade, subduction interface mélanges and/or layers of hydrated mantle wedge gained importance as fluid and element reservoirs for arcs (Iwamori, 1998; Bebout and Barton, 2002; Hyndmann and Peacock, 2003; Savov et al., 2005; Bebout, 2007, 2014; Marschall and Schumacker, 2012; Scambelluri and Tonarini, 2012; Spandler and Pirard, 2013). The Cima di Gagnone mélange consists of ultramafic bodies embedded in metasedimentary host rocks: metaperidotites host layers and dykes of MORB-type eclogite-metarodingite and show geochemical features pointing to pre-eclogitic serpentinization (Evans and Trommsdorff, 1978; Evans et al., 1979; Scambelluri et al., 2014). For this reason here we adopt the Erro-Tobbio high-pressure serpentinized peridotite as reference protolith of the Gagnone metaperidotites. The Erro-Tobbio unit (Ligurian Western Alps) derives from subcontinental mantle lithosphere firstly exhumed close to the ocean floor during rifting and opening of the Jurassic Tethys, and later involved in Alpine subduction (e.g. Hoogerduijn Strating et al., 1993; Scambelluri et al., 1995). During this evolution peridotites underwent low- (chrysotile-lizardite) and high-temperature (antigorite) serpentinization followed by formation of metamorphic olivine during eclogite-facies partial deserpentinization and fluid release (Scambelluri et al., 1995). The Erro-Tobbio serpentinization has been recently related to infiltration of slab fluids when the peridotite was in a supra-subduction or in a plate-interface setting (Scambelluri and Tonarini, 2012). In order to have fully comparable datasets, here we

Table 1
Isotopic data from Cima di Gagnone suite rocks and Erro-Tobbio serpentinites.

	Sample	B (ppm)	$\delta^{11}B$ (‰)	2σ	$^{87}Sr/^{86}Sr_{corr}$	2σ	$^{206}Pb/^{204}Pb_{corr}$	$^{207}Pb/^{204}Pb_{corr}$	$^{208}Pb/^{204}Pb_{corr}$
Ultramafic rocks									
Garnet peridotite	MG 160 09-10	8.6	−4.8	±1.9	0.712439	±9	18.548	15.671	38.866
	MG 160 09-10G	2.6	−3.3	±1.2	0.712389	±9	18.566	15.644	38.758
	MG 160 4/8	4.1	−3.9	±0.8	0.711409	±6	18.662	15.674	38.801
	MG 160 96-2	2.4	−3.0	±1.4	0.711447	±8	18.645	15.679	38.855
	MG 161 92-1	4.1	−8.6	±1.4	0.711195	±6	18.716	15.751	39.125
Chlorite harzburgite	MG 304 92-1	3.8	−5.2	±0.5	0.710867	±8	18.292	15.617	38.170
	MG 304 92-2	3.1	−7.8	±0.7	0.710844	±9	18.790	15.624	38.432
	MG 31 09-06	6.6	−7.1	±0.7	0.709034	±6	18.740	15.667	38.574
	MG 163 09-07	5.4	−9.3	±0.4	0.710631	±15	18.837	15.640	38.604
Dunite	MG 163 12-03	8.9	−4.4	±0.8	0.708964	±10	18.548	15.647	38.442
Mafic rocks									
Eclogite	MG 163 12-10	5.7	−1.6	±0.8	0.708436	±6	18.519	15.660	38.563
Garnet amphibolite	MG 163 12-11	6.1	−4.5	±0.7	0.709536	±7	18.788	15.677	38.823
Metarodingite	MG 31 12-07	6.8	−6.6	±1.0	0.707299	±9	18.553	15.652	38.520
Blackwall	MG 31 12-08	8.7	−8.0	±0.5	0.707894	±7	18.940	15.690	38.788
Country rocks									
Micaschist	MG 160 12-04	16.1	−7.7	±0.4	0.717198	±7	18.894	15.671	39.240
Gneiss	MG 31 12-01	11.4	−7.1	±0.9	0.728659	±7	18.751	15.681	39.060
	MG 31 12-02	6.9	−3.5	±1.2	0.725575	±6	18.743	15.668	39.084
	MG 163 12-17	11.3	−12.4	±0.3	0.721081	±14	18.913	15.658	38.781
	MG 163 12-18	9.4	−11.6	±0.4	0.711242	±8	18.978	15.658	38.673
Erro-Tobbio serpentinites (Ligurian Western Alps)									
HP mylonitic	ETA51	35.5*	20*	–	0.706040*	–	18.514	15.590	38.457
	ETF6	14.7*	17.9*	–	0.705147*	–	18.424	15.796	38.620
HP underformed	ETA75/A	27.3*	11.2*	–	0.704825*	–	18.402	15.565	38.260
Low-grade	ETA46	22.7*	23.3*	–	0.705560*	–	18.300	15.533	38.144

* Data from Scambelluri and Tonarini (2012).

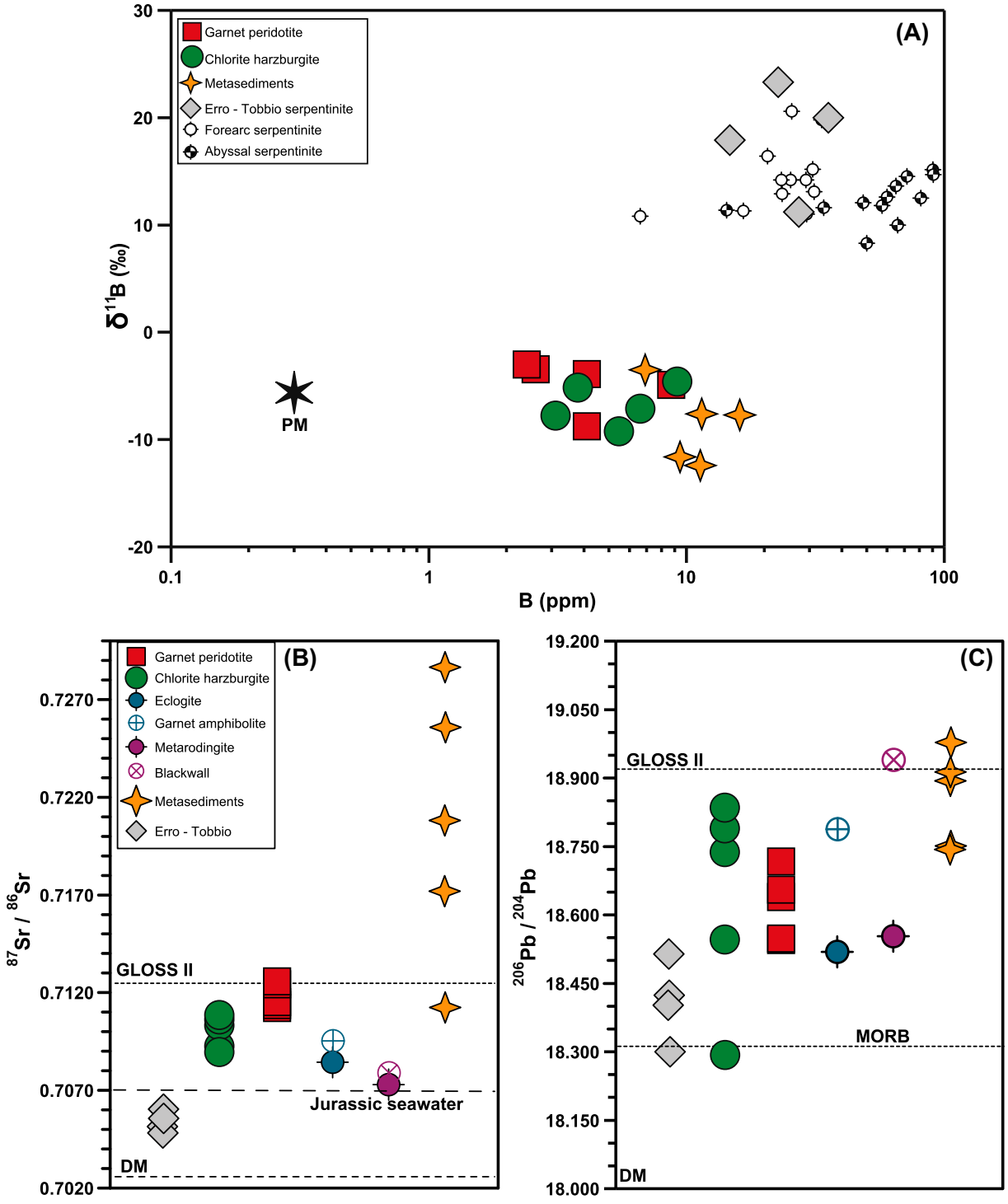

Fig. 5. Isotopic composition of the Gagnone mélange and from high pressure serpentinites of the Erro-Tobbio (Western Ligurian Alps; $\delta^{11}B$, B content and Sr isotope from Scambelluri and Tonarini, 2012). (A) $\delta^{11}B$ vs B content for the Gagnone mélange suite rocks. Due to the derivation from serpentinized mantle rocks for the garnet peridotites and chlorite harzburgite, high pressure, abyssal and forearc serpentinites are reported for comparison (Savov et al., 2005, 2007; Boschi et al., 2008; Scambelluri and Tonarini, 2012). (B) Sr isotope composition for the ultramafic rocks are higher with respect the depleted mantle (DM from Rehkamper and Hofmann, 1997), high pressure serpentinite from the Erro-Tobbio and Jurassic seawater values, suggesting an interaction with the host metasediments. Value of GLOSS II is reported for comparison (Plank, 2014). (C) $^{206}Pb/^{204}Pb$ isotope show high values and suggest an interaction between ultramafic and crustal reservoirs. Depleted mantle (DM) are from Rehkamper and Hofmann (1997), GLOSS II from Plank (2014), MORB from Klein (2003).

present new Pb isotope analyses for Erro-Tobbio, along with previous B and Sr isotope data (Table 1; Scambelluri and Tonarini, 2012).

In the Gagnone peridotite, enrichment in As, Sb and Be of the high-pressure minerals has been attributed to interaction with sediment-derived fluids during mélange formation (Scambelluri et al., 2014). By establishing the geochemical signature of the various rock types and by applying B, Sr and Pb isotopic systems, we aim at clarifying the elemental transfer between (meta)-sedimentary matrix and ultramafic blocks in the Gagnone mélange. This enables to define mass transfer in plate-interface subduction mélanges (e.g. King et al., 2006, 2007; Ague, 2007; Bebout, 2007; Marschall and Schumacker, 2012) and to identify the type of fluids released during dehydration of serpentinite from mélange formations. Since the Gagnone ultramafic rocks record input of sediment-derived fluid during prograde subduction, they may also represent proxies of supra-subduction-zone mantle metasomatized by slab fluids.

Before entering the details of isotopic tracers, key discussion points are (1) understanding tectonic coupling of sediments with ultramafic bodies by assessing P-T conditions of eclogitic metamorphism, and (2) defining mass transfer and trace element exchange between ultramafic–mafic blocks and host metasediments. These serve as a basis to assess the isotopic composition of the different systems and (3) to evaluate possible links between the Gagnone-type metaperidotite and several modern arcs.

6.1. P-T conditions, coupling of ultramafic–mafic rocks with metasediment in the Gagnone mélange

Thermobarometry of metaperidotite, eclogite, metarodingite from Gagnone and of metasediments from other areas of the Adula nappe has been performed by several authors. Garnet peridotite yields 740–800 °C and 2.0–3.0 GPa (Evans and Trommsdorff, 1978; Pfiffner, 1999; Nimis and Trommsdorff 2001): minimum temperature of 800 °C and maximum 3.0 GPa pressure (Fig. 6) have been achieved combining geothermometry with phase diagram sections (Scambelluri et al., 2014). Pseudosections for Ca-bearing chlorite harzburgite suggest temperatures of maximum 720 °C for the peak olivine + orthopyroxene + chlorite paragenesis; a maximum temperature of 800 °C is inferred for Ca-free compositions (Fig. 6; Scambelluri et al., 2014).

The Gagnone eclogite and metarodingite are hosted in the chlorite harzburgite lenses. According to Evans et al. (1979), eclogite records 800 °C and 2.5 GPa. The garnet-pyroxene calibration (Ellis and Green, 1979) applied to our eclogite and metarodingite samples (see Electronic Appendix 1; Tables A2 and A3) provides peak conditions of 780–800 ± 50 °C for 2.0–2.5 GPa (Fig. 6).

Concerning the Gagnone paraschists, core-to-rim variations in the Si content of phengite relics (3.36–3.20 to 3.13–3.06 Si p.f.u.; Fig. 3C) are comparable with values of Pfiffner (1999; up to 3.37 Si p.f.u.) and reflect a change in pressure conditions. Adopting a 700–800 °C temperature range, the Caddick and Thompson (2008) calibration yields pressures of 2.1 ± 0.2 GPa (Fig. 6; see Electronic Appendix 1 and Table A4), i.e. below the P–T conditions of wet partial melting for this system (Auzanneau et al., 2006). Our data are consistent with P-T estimates for other Adula localities (3.45 to 3.38 p.f.u. Si in phengite), yielding pressure of 1.9–2.5 GPa at lower temperature (650 °C, Meyre et al., 1999).

The similarity of P-T conditions recorded by the different Gagnone rock-types (Fig. 6) points to a common eclogite-facies equilibration for country rocks and ultramafic-eclogitic blocks at Gagnone, and indicates accretion into the present-day mélange during prograde and/or peak metamorphism. The lower pressure recorded by the country paragneiss can be due to retrograde re-equilibration of phengitic mica. Importantly, the peak pressure–temperature conditions achieved for Gagnone metaperidotite (Fig. 6) correspond to top-slab temperatures at sub-arc depths reproduced in thermal models (D80 model from Syracuse et al., 2010). Therefore, the eclogite-facies metamorphism and the deserpentinzation process recorded by the Gagnone metaperidotites can be representative of subarc environments. In the next sections we discuss the geochemical effects related to the early accretion of ultramafic rocks into the mélange and to their dehydration under eclogite-facies conditions.

6.2. Mass transfer and elemental exchange between ultramafic - mafic bodies and host rocks

The Sr and Pb ratios of peridotites and eclogite are higher than depleted mantle (DM) and MORB protoliths and provide evidence of interaction between country rocks and ultramafic–mafic bodies (Fig. 5B and C). Although pre-subduction oceanic alteration by seawater was proposed according to field and trace element evidence (Evans and Trommsdorff, 1978; Scambelluri et al., 2014), our dataset shows that the Sr and Pb isotopic compositions of ultramafic and mafic rocks were reset towards crustal values during exchange with the mélange matrix in the subduction setting (Fig. 5B and C). Besides Pb and Sr, the exchange process likely brought into ultramafic rocks fluid-mobile elements such as B, Pb, U, Th, As and Sb (Scambelluri et al., 2014). The process is visualized in Fig. 7, reporting the PM-normalized (McDonough and Sun, 1995) bulk-rock contents in As and Sb of samples collected along profiles from peridotite lenses to country gneiss in two outcrops of chlorite harzburgite (MG31 and MG163; Figs. 1, 2 and 7A and B) and in one garnet peridotite body (MG160; Fig. 1, Fig. 7C). Compared to a pelitic protolith, the Gagnone paraschist is depleted in As, Sb (and, in minor amount, in B). This variable depletion is coupled with increase of the same elements (above PM, MORB and subducted serpentinite concentrations) in chlorite harzburgite, in the associated eclogite-metarodingite (Fig. 7A and B), and in garnet peridotite (Fig. 7C). These features indicate element exchange between host metasediments and ultramafic lenses, together with re-equilibration of metaperidotite and mafic rocks towards crustal values.

The trace element patterns of the high-pressure minerals from chlorite harzburgite and garnet peridotite shown in Fig. 7D and E (in-situ LA-ICPMS analyses from

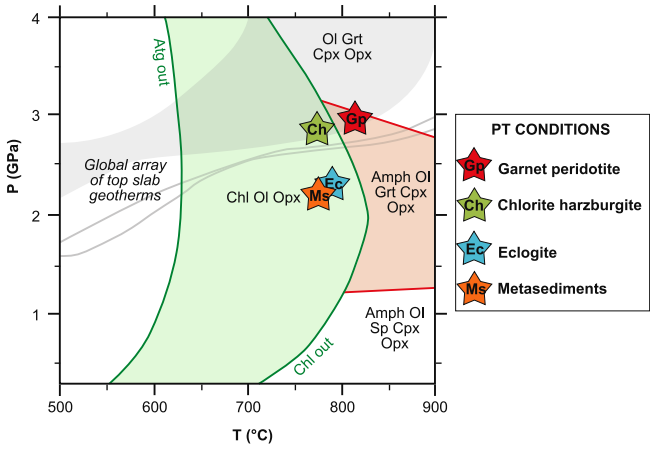

Fig. 6. Stability fields of the high pressure assemblage for chlorite harzburgite (in green) and for garnet peridotite (in red) based on pseudosections calculation from Scambelluri et al. (2014). Stars represent pressure–temperature conditions estimated for the Gagnone mélange suite rocks. Note that metaperidotite conditions partially overlap the global array of top slab geotherms (in gray) of the D80 model of Syracuse et al. (2010). (For interpretation of the references to color in this figure legend, the reader is referred to the web version of this article.)

Scambelluri et al., 2014) are characterized by positive anomalies in B, Pb, As, Sb, indicating that the enrichment in such fluid-mobile elements pre-dated peak metamorphism. The involvement of fluid-mobile elements like As and Sb, transported at relatively low-temperature (Deschamps et al., 2011; Lafay et al., 2013), suggests that tectonic accretion of ultramafic slices to the sedimentary veneer should have occurred since the early stages of subduction. The B, Pb, As, Sb and Sr mobility could be explained by sediment compaction and pore-fluid expulsion during low-temperature early burial, as documented in other mélange settings (e.g. Bebout et al., 1999; Deschamps et al., 2011). Such fluids may either interact with serpentinite slices in the sedimentary veneer, or flush the overlying mantle (Benton et al., 2001; Hattori and Guillot, 2003, 2007; Savov et al., 2005, 2007; Deschamps et al., 2011, 2012; Debret et al., 2013; Lafay et al., 2013; Barnes et al., 2014). The geochemical fingerprint of ultramafic rocks from Gagnone can thus approximate the above general cases.

The fluid-mediated exchange affecting the Gagnone peridotites has been further monitored with boron isotopes. To date, B is considered an excellent tracer of fluid transfer from slabs to arcs (Rosner et al., 2003; Tonarini et al., 2005, 2007), its main source being identified in serpentinized mantle reservoirs (Tonarini et al., 2011; Scambelluri and Tonarini, 2012). The Gagnone case-study presented here, helps to define: (1) the B isotopic composition of ultramafic rocks affected by interaction with externally derived fluids; (2) the fingerprints of the fluids produced, potentially affecting arc magmas, and the composition of dehydrated rock residues returned to the deep mantle.

The available data indicate that serpentinites have high B contents (10–100 ppm) and positive $\delta^{11}B$ (10–25‰, Fig. 5A; Savov et al., 2005, 2007; Boschi et al., 2008). Compared with precursor serpentinites, the Gagnone chlorite harzburgite, dunite and garnet peridotite have lower B and negative $\delta^{11}B$ (Table. 1; Fig. 5A). A process that can be invoked to explain decrease in bulk B and enrichment in ^{10}B isotope in the Gagnone peridotites is fractionation during dehydration, as documented for altered oceanic crust (Rosner et al., 2003; Tonarini et al., 2005; King et al., 2007; Pabst et al., 2012). However, several authors suggest that closed-system dehydration under high-temperature ($T > 600$ °C, 2 GPa) and the basic pH of serpentinite fluids (about 12.6 pH) potentially minimize boron isotope fractionation, producing dehydrated peridotites with positive $\delta^{11}B$ (Palmer and Swihart, 1996; Mottl et al., 2003; Scambelluri and Tonarini, 2012). One possible explanation of the low B and of the negative $\delta^{11}B$ values of the Gagnone peridotites (Fig. 5A) is a combined effect of serpentine dehydration (decreasing B and to some extent the ^{11}B content of rocks) and interaction with negative $\delta^{11}B$ fluids sourced by metasediments (Ishikawa and Nakamura, 1994; Ishikawa and Tera, 1999; Nakano and Nakamura, 2001; Bebout and Nakamura, 2003, Tonarini et al., 2011). In a $\delta^{11}B$ vs B/Nb diagram (Fig. 8A), the Gagnone peridotites fall along a theoretical mixing line between the ^{11}B-rich Erro-Tobbio high-pressure serpentinites and host metasediments. Same as the Pb and Sr isotopes (Fig. 5B and C), the B isotopes thus suggest that interaction with sediment-derived fluids affected the Gagnone peridotite signature.

Here we propose that the geological context is relevant and that decrease in $\delta^{11}B$ of ultramafic rocks, especially those evolved in subduction settings, must be tested taking into account contamination from ^{11}B poor reservoirs.

The $^{87}Sr/^{86}Sr$ vs $^{206}Pb/^{204}Pb$ diagram of Fig. 8B shows the effects of superposed fluid-rock interaction episodes recorded by the Gagnone rock suite and enables to distinguish the effects of retrograde fluid overprint on the geochemical signature acquired during peak metamorphism. The diagram shows the isotopic composition of the entire sample suite, characterized by a large range of $^{206}Pb/^{204}Pb$ (18.292-19) and $^{87}Sr/^{86}Sr$ ratios (0.70729–0.721081). This heterogeneity can be explained by means of superposed fluid-rock interactions affecting the samples.

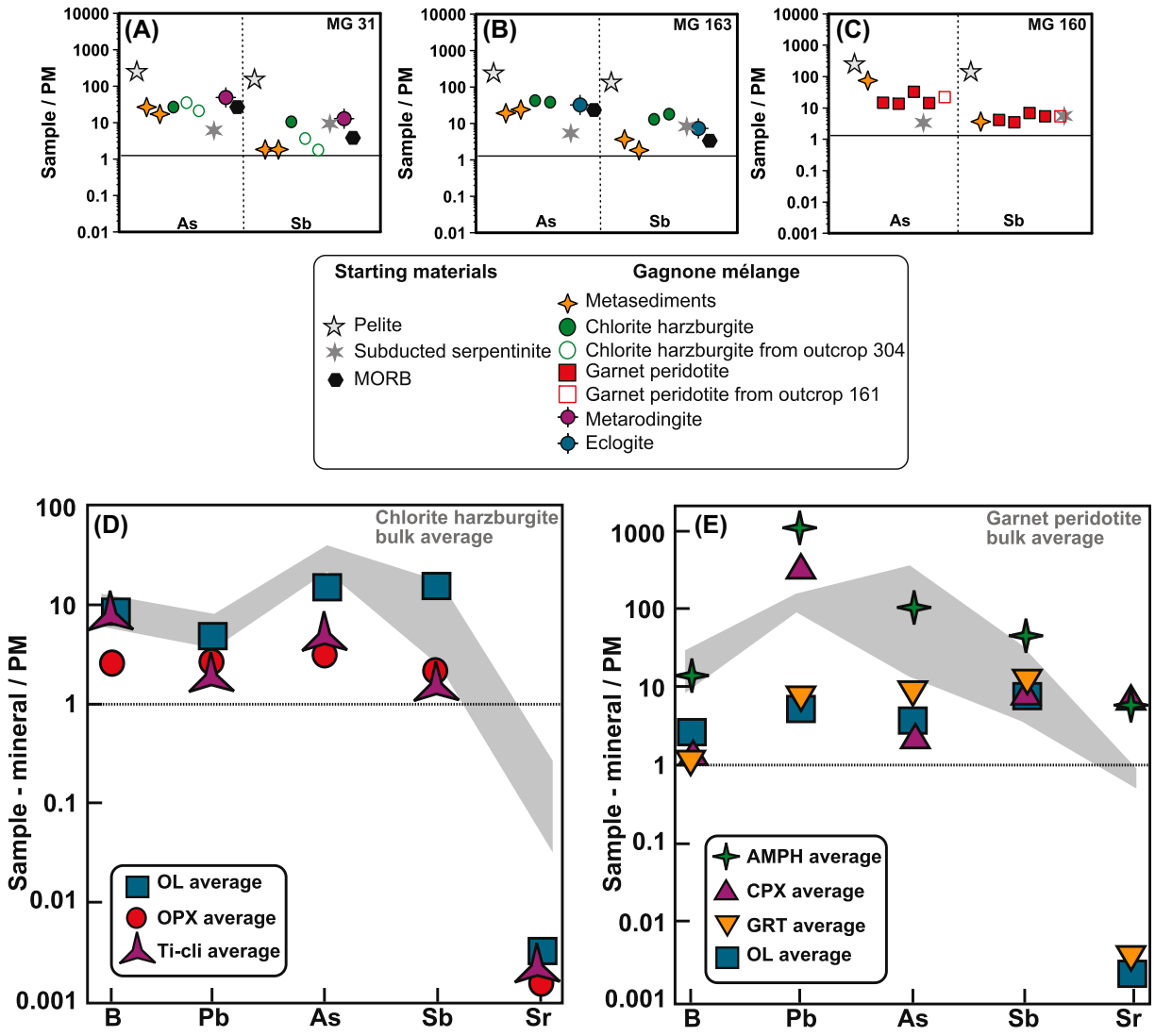

Fig. 7. Relative variations in As and Sb in the Gagnone mélange suite rocks for the main chlorite harzburgite outcrop MG 31 (A) and MG 163 (B) and garnet peridotites one MG 160 (C) normalized to primitive mantle values (McDonough and Sun, 1995). In (A) are also reported the chlorite harzburgite samples from the outcrop MG 304 and in (C) the garnet peridotite from outcrop MG 161 (open symbols). For comparison are reported also the values of the starting materials: pelite, subducted serpentinites and MORB (Onishi and Sandell (1955) and Jochum and Hofmann (1997) for As and Sb values in MORB, respectively; Li (1991) for pelite; Deschamps et al., 2011 for subducted serpentinites). The depletion in As and Sb in the metasediment are associated to the enrichment in the metaperiodate indicating exchange between them at relative low temperature. (D) and (E) Enrichment in FME, with respect to the primitive mantle, in the chlorite harzburgite and garnet peridotites whole rock (grey field) and in their high pressure minerals, support the hypothesis of prograde to peak exchange from the metasedimentary matrix rocks to the ultramafic (and mafic) bodies. As shown by Scambelluri et al. (2014) the mineral assemblages play a role of primary relevance concerning the enrichment in some elements like Sr and Pb that show a compatible behavior in peridotite-bearing rocks, like clinopyroxene and amphibole. (OL: olivine, OPX: orthopyroxene, Ti-cli: Ti-clinohumite, AMPH: amphibole, CPX: clinopyroxene, GRT: garnet).

In Fig. 8B, the $^{206}Pb/^{204}Pb$ ratios of one group of garnet peridotite, chlorite harzburgite and high-pressure mafic rocks plots between 18.29 and 18.66. These samples fall along three mixing lines between the Erro-Tobbio high-pressure serpentinized peridotite and the paragneiss samples from outcrop MG31 (with highest $^{87}Sr/^{86}Sr$ and low $^{206}Pb/^{204}Pb$, and preserving significant modal amounts of eclogite-facies minerals). The mixing lines display the possible changes in isotopic composition during interaction of the Erro-Tobbio protolith with a fluid sourced by the high-pressure MG31 paragneiss. The mixing lines were calculated using sample ETA46 as serpentinized Erro-Tobbio protolith (with low $^{206}Pb/^{204}Pb$ and $^{87}Sr/^{86}Sr$ ratios; Table 1). The Pb and Sr isotopic composition of the metasediment-derived fluid driving the mixing process virtually corresponds to the composition of the MG31 paragneiss, due to a lack of radiogenic isotope fractionation during fluid release. Calculation of the mixing lines of

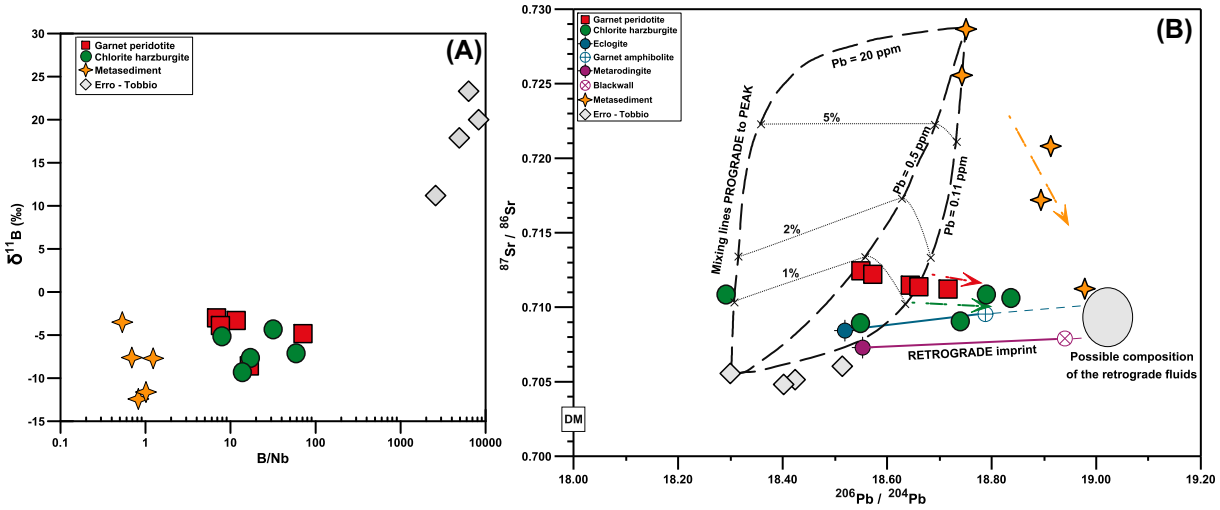

Fig. 8. (A) In a $\delta^{11}B$ vs B/Nb ratio plot ultramafic rocks fall in between the high pressure serpentinized rocks and the Gneiss and Micaschist of Gagnone. A possible interaction between these end-member reservoirs seem occurred during subduction processes. (B) Mixing lines (with different Pb content in the protolith, see Appendix A-1 for input parameters of the mixing models) in a $^{87}Sr/^{86}Sr$ vs $^{206}Pb/^{204}Pb$ plot show prograde to peak interaction between high pressure ultramafic rocks and crustal reservoirs. The degree of interaction is also reported along the three different mixing lines (1–2–5%). Ultramafic samples show 1–2% degree of interaction with crustal component. Retrograde imprint leading higher Pb isotope ratio is also visible in particular with the blackwall and garnet-bearing amphibolite mafic rocks. The retrograde field is individuate by the intersection of the retrograde trends shown by all lithologies. Note that the composition of the retrograde fluids is quite different from those of the prograde/peak one. Depleted mantle (DM) value from Rehkamper and Hofmann (1997).

Fig. 8B also requires the Sr and Pb concentrations in the reacting rock and fluid. For this purpose we have employed the measured Sr and Pb concentrations in ETA46 (Table A1): we have also considered additional arbitrary Pb values of 0.5 and 20 ppm. The Pb and Sr contents of the fluid have been achieved using the concentrations measured in samples MG31 (Table A1) and applying the fluid/rock partition coefficients for Sr and Pb of Leeman (1996). Further detail on the calculations and on the equation employed is provided in the Electronic Appendix 1. The three mixing lines intercept four garnet peridotites, one chlorite harzburgite, the dunite, the preserved eclogite (MG163 12-10) and metarodingite (MG31 12-07). The degrees of interaction individuated by the model (1%, 2% and 5% in Fig. 8B) suggest a maximum of 2% crustal component added to these rocks by the fluid. The $^{206}Pb/^{204}Pb$ ratios of samples showing higher amounts of retrograde minerals (amphibolitized eclogite MG163 12-11; metarodingite blackwall MG31 12-08; garnet peridotite MG 161 92-1; chlorite harzburgites MG304 92-2, MG31 09-07, MG163 09-07) shift towards values as high as 19.0 and about 0.71 of $^{87}Sr/^{86}Sr$ (and also $\delta^{11}B = -10‰$, see Table 1). We relate this shift to retrograde fluid infiltration (arrows in Fig. 8B) enhancing partial re-equilibration of the Pb and Sr isotopic signatures acquired during prograde interaction between host metasediments and ultramafic–mafic bodies. We therefore interpret the isotopic compositions of samples plotting close to the dashed mixing lines of Fig. 8B as acquired during prograde to peak exchange in the subduction interface mélange of Gagnone.

In summary, the Gagnone case study can serve as a guideline to understand peridotite and serpentinized peridotite contamination during interaction with sediment-derived fluids in subduction settings. We think this context is relevant, as it may disclose the exchange processes between two rock systems that largely control the water and fluid-mobile element budgets for subduction. This interaction is not only representative of mélange settings; it can also play a role when considering hydration of forearc mantle by uprising slab fluids. Our petrologic background and isotopic dataset is hereafter used to define the potential role of Gagnone-type metaperidotites in element recycling to arcs.

6.3. Global processes: link between peridotites from Cima di Gagnone and arc magmatism

It is now accepted that the genesis of arc lavas is related to element and H_2O–CO_2 fluid input at subduction zones. The direct link between subduction input and volcanic arc output established by numerous authors is reflected by distinctive LILE enrichment and by volatile-rich compositions of arc magmas with respect to unaltered mantle values (e.g. Ringwood, 1974; Moran et al., 1992; Leeman, 1996; Elliott, 2003; Hattori and Guillot, 2003; Rosner et al., 2003; Breeding et al., 2004; Tonarini et al., 2005, 2007, 2011; King et al., 2007; Scambelluri and Tonarini, 2012; Spandler and Pirard, 2013). In particular, the significant enrichment in arc lavas of LREE and LILE preferentially hosted in sediments has long suggested the direct involvement of sedimentary materials and altered oceanic crust in fluid and element loss from slabs at subarc depths (e.g. Bebout et al., 1999; Peacock and Hervig, 1999; Rosner et al., 2003; Tonarini et al., 2005). However, a number of recent works provided different views of the transfer process, suggesting that hydrated (serpentinized) mantle rocks

from the slab or from the supra-subduction hanging wall mantle are relevant to fluid and element transfer to depth and delivery to arcs. The general transfer mechanism is not fully understood. Some authors suggest sub-arc slab dehydration through the interplay of serpentinite dehydration and fluid interaction with different slab layers to mobilize the elements (e.g. Bebout, 2007; Spandler et al., 2008). Others propose that the hanging wall mantle wedge fixes and transports to depth the fluids and elements uprising from the slab (e.g. Hyndman and Peacock, 2003; Savov et al., 2005; Scambelluri and Tonarini, 2012). A third class of models suggests the diapiric uprise of buoyant plate-interface serpentinite and/or mélange layers into the mantle wedge and their direct melting in hot subarc mantle regions (Gerya et al., 2002; Behn et al., 2011; Marschall and Schumacker, 2012). The correspondence of peak pressure–temperature estimates for the Gagnone mélange with subarc conditions suggested by thermal models (Fig. 6; Syracuse et al., 2010) and geophysical imaging of subduction zones (e.g. Bostock et al., 2002; Friederich et al., 2014) encourages the use of these rocks to understand the role of deserpentinization of Gagnone-type peridotites in affecting the isotopic signature of arc lavas (Figs. 9 and 10).

Fig. 9A reports the $\delta^{11}B$ and Nb/B compositions of the Gagnone metaperidotite samples less affected by retrograde re-equilibration (Fig. 8B), together with reference mantle, high-pressure Erro-Tobbio serpentinite and metasediments. The dashed line connecting Erro-Tobbio serpentinite and sedimentary end-members (line 1) represents hypothetical serpentinite-sediment mixed reservoir, whose compositions depend on the amount of end-members involved. For example, addition to the mantle source of a relatively pure serpentinite fluid, as may occur in sediment-poor ocean-ocean convergent margins, leads to production of magmas like the South Sandwich Island arc (SSI in Fig. 9A; mixing line 2: for mixing model parameters refer to Scambelluri and Tonarini, 2012). Addition of a fluid sourced by a metasomatized Gagnone-type component (e.g. dashed line 3) can generate a number of arc lavas with low to negative $\delta^{11}B$, representative of convergent margins with larger amounts of sediment involved (e.g. Andes, El Salvador, Kurile, Phlegrean volcanic district, Turkey, Aleutian, Cascades). Comparable features are shown by the $\delta^{11}B$ vs $^{87}Sr/^{86}Sr$ diagram of Fig. 9B, suggesting that adding a serpentinite component to the mantle (dashed line 2) generates the SSI arc lavas. If a Gagnone-type component is mixed to the mantle along dashed line 3, the corresponding arc lavas have higher radiogenic Sr component. Note that to form the latter lavas, addition of a fluid component directly sourced by sediments at subarc settings (plotting in Fig. 9B at high $^{87}Sr/^{86}Sr$ and negative $\delta^{11}B$ values) is not necessary. We envisage a transfer process schematically represented in Fig. 10, which requires fluid-mediated exchange between sedimentary reservoirs and serpentinized mantle, and subsequent dehydration of the metasomatized serpentinized mantle. This process may occur in mélange settings such as Gagnone (Fig. 10A), by means of hydration of supra-subduction mantle followed by fluid release upon serpentinite dehydration, or by diapiric uprise of mélange materials (Fig. 10B). Our isotopic study thus supports a model with serpentinite acting as sink and carrier of fluid-mobile elements, as previously suggested by a number of studies (Ryan et al., 1995, 1996; Savov et al., 2007; Deschamps et al., 2011; Scambelluri

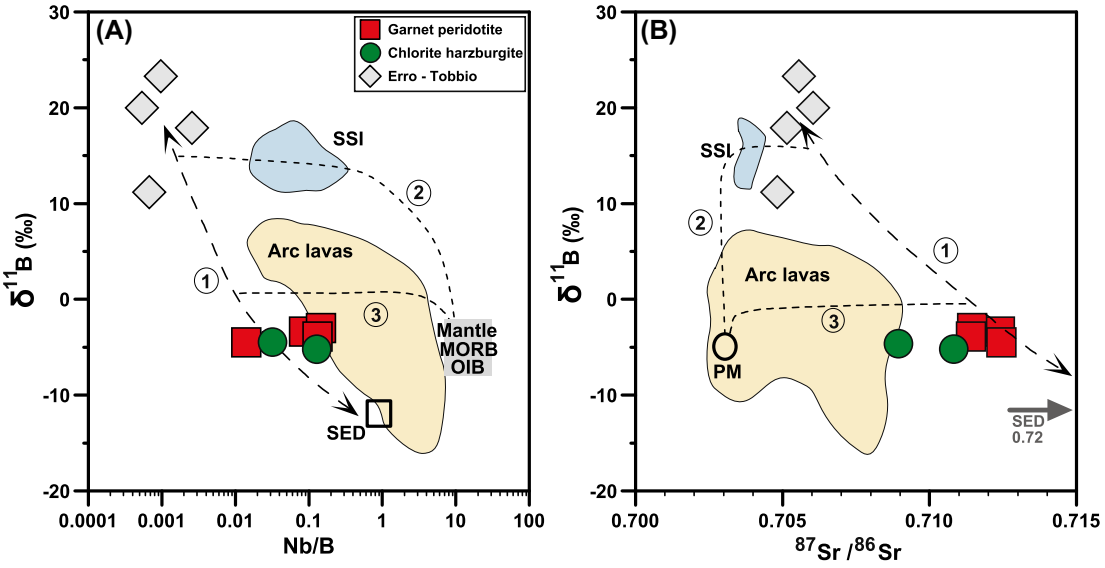

Fig. 9. A) $\delta^{11}B$ vs Nb/B ratio and B) $\delta^{11}B$ vs $^{87}Sr/^{86}Sr$ isotopes plot show the major geochemical implications of the interaction processes at the plate interface environment in arc magma genesis. Early elements exchange from sediment/crustal to ultramafic rocks allow ultramafic rocks to become reservoir enable them to acquire sedimentary geochemical fingerprint that moves along the dashed line number 1. Uprising fluids from dehydration of serpentine pure component provide geochemical anomalies in the above mantle as show by the South Sandwich Island lavas (SSI; mixing line number 2; data from Tonarini et al., 2011). Dehydration of ultramafic rocks after exchange (dashed line number 3) supply geochemical heterogeneities observed for all other arc lavas. Arc lavas fields from Scambelluri and Tonarini (2012, and references therein). SED: sediments.

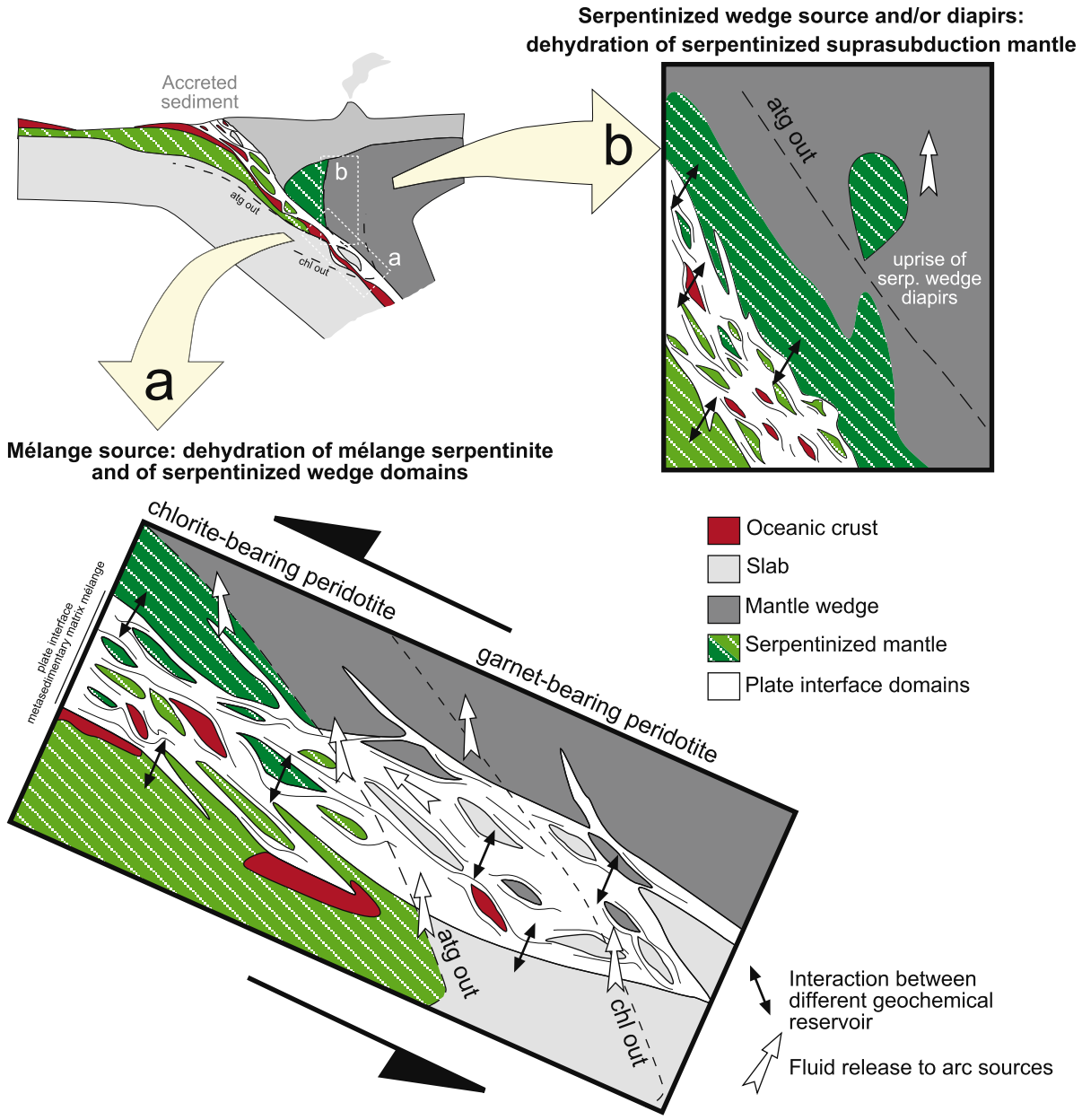

Fig. 10. Schematic model of interaction between different geochemical reservoirs at the plate interface environment and main geochemical implications (redrawn after Trommsdorff, 1990). (A) Release of fluids from mélange source and dehydration of mélange serpentinites and of serpentinized wedge could triggering the arc magmatism and could explain the geochemical anomalies characteristic of many arc lavas; (B) geochemical anomalies into arc magma source introduced by uprise of serpentinized wedge diapirs due to their low density compared to the surrounding materials.

and Tonarini, 2012; Lafay et al., 2013; Ryan and Chauvel, 2014).

7. CONCLUSIONS

The Gagnone high-pressure mélange consists of metaperidotite bodies including eclogite and metarodingite, embedded in metasediments forming the mélange matrix. These rocks recrystallized at pressure–temperature conditions corresponding to sub-arc depths according to recent thermal models of subduction zones (Syracuse et al., 2010).

Metaperidotite derives from deserpentinization of hydrated mantle rocks and shows clear evidence of elemental exchange with the metasedimentary mélange matrix. Ultramafic and associated mafic rocks are enriched in fluid-mobile As, Sb and B, display high contents in radiogenic Sr and Pb, and have negative $\delta^{11}B$: these features indicate exchange with metasediments and reset of the pre-subduction isotopic signatures.

To explain the fluid-mediated change of the Gagnone metaperidotites towards sedimentary values we propose the exchange with fluids that interacted with the host

metasediments during subduction burial. The transfer process pre-dated peak metamorphism and dehydration of the ultramafic rocks at sub-arc depths.

Importantly, the isotopic fingerprint of the Gagnone peridotites may explain the genesis of a number of arc lavas requiring input of sedimentary components to their mantle source, without direct involvement of sediment dehydration/melting at subarc depths.

We suggest that investigating the sources of "*slab signatures*" in arc lavas requires to more throughly consider mixing of the type demonstrated here. Various mixtures of sediment, oceanic crust, and ultramafic signatures need not be attributed to multiple fluids, and can instead be the result of geochemical mixing of different key lithologies. The process envisaged here is element transfer from sediment to serpentinized peridotite, followed by peridotite dehydration and release of de-serpentinization fluids conveying inherited sedimentary components into the mantle wedge.

ACKNOWLEDGEMENT

This research is funded by the Italian MIUR (PRIN-COFIN project 2012R33ECR_002 *Volatile transfer at convergent plate margins: linking COH fluids/melts heterogeneities to tectonic anomalies in subduction zones*). We thank Andrea Risplendente and Laura Negretti for technical assistence during microprobe analysis and scanning electron microscopy. Jaime Barnes, Gray Bebout, an anonymous reviewer and the GCA editor Clark M. Johnson are gratefully acknowledged for insightful comments that significantly improved the focus of this paper.

APPENDIX A. SUPPLEMENTARY DATA

Supplementary data associated with this article can be found, in the online version, at http://dx.doi.org/10.1016/j.gca.2015.04.024.

REFERENCES

Ague J. J. (2007) Models of permeability contrasts in subduction zone mélange: implications for gradients in fluid fluxes, Syros and Tinos Islands, Greece. *Chem. Geol.* **239**, 217–227.

Angiboust S., Pettke T., De Hoog J. C. M., Caron B. and Oncken O. (2014) Channelized fluid flow and eclogite-facies metasomatism along the sunduction shear zone. *J. Petrol.* **55**, 883–916.

Auzanneau E., Vielzeuf D. and Schimdt M. W. (2006) Experimental evidence of decompression melting during exhumation of subducted continental crust. *Contrib. Mineral. Petrol.* **152**, 125–148.

Barnes J. D., Beltrando M., Lee C. A., Cisneros M., Loewy S. and Chin E. (2014) Geochemistry of Alpine serpentinites from rifting to subduction: a view across paleogeographic domains and metamorphic grade. *Chem. Geol.* **389**, 29–47.

Bebout G. E. (2007) Metamorphic chemical geodynamics of subduction zones. *Earth Planet. Sci. Lett.* **260**, 373–393.

Bebout G. E. (2014) Chemical and isotopic cycling in subduction zones. Chapter 4.20: The crust. In *Treatise on Geochemistry* (ed. R. Carlson), second ed. pp. 703–747.

Bebout G. E. and Barton M. D. (2002) Tectonic and metasomatic mixing in a high-T, subduction-zone mélange-insights into the geochemical evolution of the slab-mantle interface. *Chem. Geol.* **187**, 79–106.

Bebout G. E. and Nakamura E. (2003) Record in metamorphic tourmalines of subduction-zone devolatilization and boron cycling. *Geology* **31**(5), 407–410.

Bebout G. E., Ryan J. G. and Leeman W. P. (1993) B-Be systematics in subduction-related metamorphic rocks: Characterization of the subducted component. *Geochim. Cosmochim. Acta* **57**, 2227–2237.

Bebout G. E., Ryan J. G., Leeman W. P. and Bebout A. E. (1999) Fractionation of trace elements during subduction-zone metamorphism: impact of convergent margin thermal evolution. *Earth Planet. Sci. Lett.* **171**, 63–81.

Becker H. (1993) Garnet peridotite and eclogite Sm-Nd mineral ages from the Lepontine dome (Swiss Alps): new evidence for Eocene high-pressure metamorphism in the Central Alps. *Geology* **21**, 599–602.

Behn M. D., Kelemen P. B., Hirth G., Hacker B. R. and Massonne H. J. (2011) Diapirs as the source of the sediment signature in arc lavas. *Nat. Geosci.* **4**, 641–646.

Benton L. D., Ryan J. G. and Tera F. (2001) Boron isotope systematic of slab fluids as inferred from a serpentinite seamount, Mariana forearc. *Earth Planet. Sci. Lett.* **187**, 273–282.

Berger A. and Bousquet R. (2007) Subduction related metamorphism in the Alps: review of isotopic ages based on petrology and their geodynamic consequences. *Geol. Soc. Lond. Spec. Publ.* **298**, 117–144.

Boschi C., Dini A., Frueh Green G. L. and Kelley D. S. (2008) Isotopic and element exchange during serpentinization and metasomatism at the Atlantis Massif (MAR 308N): insights from B and Sr isotope data. *Geochim. Cosmochim. Acta* **72**, 1801–1823.

Bostock M. G., Hyndman R. D., Rondenay S. and Peacock S. M. (2002) An inverted continental Moho and serpentinization of the forearc mantle. *Nature* **417**, 536–538.

Breeding C. M., Ague J. J. and Brocker M. (2004) Fluid–metasedimentary interactions in subduction zone mélange: implications for the chemical composition of arc magmas. *Geology* **32**, 1041–1044.

Brouwer F. M., Burri T., Engi M. and Berger A. (2005) Eclogite relics in the Central Alps: regional distribution, metamorphic PT-evolution, Lu-Hf ages, and genetic implications on the formation of tectonic mélange zones. *Schweizerische Mineralogische Petrographische Mitteilungen* **85**, 147–174.

Caddick M. J. and Thompson A. B. (2008) Quantifying the tectono-metamorphic evolution of politic rocks from a wide range of tectonic setting: mineral composition in equilibrium. *Contrib. Mineral. Petrol.* **156**, 177–195.

Catanzaro E. J., Champion C. E., Garner E. L., Malinenko G., Sappenfield K. M. and Shields K. M. (1970) Boric acid: isotopic and assay standard reference materials. *US Nat. Bur. Stand. Spec. Publ.* **260–17**, 70.

Debret B., Andreani M., Godard M., Nicollet C., Schwartz S. and Lafay R. (2013) Trace element behaviour during serpentinization/de-serpentinization of an eclogitized oceanic lithosphere: a LA-ICPMS study of the Lanzo ultramafic massif (Western Alps). *Chem. Geol.* **357**, 117–133.

Deschamps F., Godard M., Guillot S., Chauvel C., Andreani M., Hattori K., Wunder B. and France L. (2012) Behavior of fluid-mobile elements in serpentines from abyssal to subduction environments: Examples from Cuba and Dominican Republic. *Chem. Geol.* **312–313**, 93–117.

Deschamps F., Guillot S., Godard M., Andreani M. and Hattori K. (2011) Serpentinites act as sponges for fluid-mobile elements

in abyssal and subduction zone environments. *Terranova* **23**, 171–178.

Deschamps F., Godard M., Guillot S. and Hattori K. (2013) Geochemistry of subduction zone serpentinites. *Lithos* **178**, 96–127.

Elliott T. R. (2003) *Inside the Subduction Factory (Geophysical Monograph 138)*. (ed. J. Eiler). American Geophysical Union, Washington, DC, pp. 23–45.

Ellis D. J. and Green D. H. (1979) An experimental study of the effect of Ca upon the garnet-clinopyroxene Fe–Mg exchange equilibria. *Contrib. Mineral Petrol.* **71**, 13–22.

Engi M., Berger A. and Roselle G. T. (2001) Role of the tectonic accretion channel in collisional orogeny. *Geology* **12**, 1143–1146.

Evans B. W. and Trommsdorff V. (1978) Petrogenesis of garnet lherzo- lite, Cima di Gagnone, Lepontine Alps. *Earth Planet. Sci. Lett.* **40**, 333–348.

Evans B. W., Trommsdorff V. and Richter W. (1979) Petrology of an eclogite-metarodingite suite at Cima di Gagnone, Ticino, Switzerland. *Am. Mineral.* **64**, 15–31.

Evans B. W., Trommsdorff V. and Goles G. G. (1981) Geochemistry of high-grade eclogites and metarodingites from the Central Alps. *Contrib. Mineral Petrol.* **76**, 301–311.

Friederich W., Lambrecht L., Stockhert B., Wassmann S. and Moos C. (2014) Seismic visibility of a deep subduction channel – insights from numerical simulation of high-frequency seismic waves emitted from intermediate depth earthquakes. *Solid Earth* **5**, 141–159.

Fumasoli M. W. (1974) Geologie des Gebietes nordlich und sudlich der Jorio-Tonale-Linie im Westen von Gravedona (Como, Italia). Dissertation thesis, Universitat Zurich, p. 230.

Gebauer D. (1996) A P-T-t path for an (ultra?-) high-pressure ultramafic/mafic rock-association and its felsic country-rocks based on SHRIMP dating of magmatic and metamorphic zircon domains. Example: Alpe Arami (Central Swiss Alps). Earth processes: reading the isotopic code. *Am. Geophys. Union, Geophys. Monogr.* **95**, 309–328.

Gebauer D., Grunenfelder M., Tilton G., Trommsdorff V. and Schmid S. (1992) The geodynamic evolution of garnet-peridotites, garnet-pyroxenites and eclogites of Alpe Arami and Cima di Gagnone (Central Alps) from early protero-zoic to oligocene. *Schweiz. Mineral. Petrogr. Mitt.* **72**, 107–111.

Gerya T. V., Stockhert B. and Perchuk A. L. (2002) Exhumation of high-pressure metamorphic rocks in a subduction channel: a numerical simulation. *Tectonics* **21**, 1–19.

Godard M., Jousselin D. and Bodinier J.-L. (2000) Relationships be- tween geochemistry and structure beneath a palaeo-spreading centre: a study of the mantle section in the Oman ophiolite. *Earth Planet. Sci. Lett.* **180**, 133–148.

Grond R., Wahl F. and Pfiffner M. (1995) Mehrphasige alpine deformation und metamorphose in der nördlichen Cima-Lunga-Einheil. Zentralalpen (Schweiz). *Schweiz. Mineral. Petrogr. Mitt.* **75**, 371–386.

Hattori K. H. and Guillot S. (2003) Volcanic fronts form as a consequence of serpentinite dehydration in the forearc mantle wedge. *Geology* **31**, 525–528.

Hattori K. H. and Guillot S. (2007) Geochemical character of serpentinites associated with high- to ultrahigh-pressure metamorphic rocks in the Alps, Cuba, and the Himalayas: recycling of elements in subduction zones. *Geochem. Geophys. Geosyst.* **8**(9). http://dx.doi.org/10.1029/2007GC001594.

Heinrich C. (1978) Metamorphise und Strukturen der Cima unga-Serie: I C. di Gagnone – Val Motto. Diploma thesis, ETH Zurich.

Heinrich C. A. (1982) Kyanite-eclogite to amphibolite facies evolution of hydrous mafic and pelitic rocks, Adula nappe, Central Alps. *Contrib. Mineral Petrol.* **81**, 30–38.

Heinrich C. A. (1986) Eclogite facies regional metamorphism of hydrous mafic rocks in the Central Alpine Adula nappe. *J. Petrol.* **27**, 123–154.

Herwartz D., Nagel T. J., Munker C., Scherer E. E. and Froitzheim N. (2011) Tracing two orogenic cycles in one eclogite sample by Lu-Hf garnet chronometry. *Nat. Geosci.* **4**, 178–183.

Hoogerduijn Strating E. H., Rampone E., Piccardo G. B., Drury M. and Vissers R. L. M. (1993) Subsolidus emplacement of mantle peridotites during incipient oceanic rifting and opening of the Mesozoic Tethys (Voltri Massif, NW Italy). *J. Petrol.* **34**, 901–927.

Hyndman R. D. and Peacock S. M. (2003) Serpentinization of the forearc mantle. *Earth Planet. Sci. Lett.* **212**, 417–432.

Ionov D. A., Savoyant L. and Dupuy C. (1992) Application of the ICP-MS technique to trace element analysis of peridotites and their minerals. *Geostand. Newsl.* **16**, 311–315.

Ishikawa T. and Nakamura E. (1994) Origin of the slab component in arc lavas from across-arc variation of B and Pb isotopes. *Nature* **370**, 205–208.

Ishikawa T. and Tera F. (1999) Two isotopically distinct fluid components involved in the Mariana arc: evidence from Nb/B ratios and B, Sr, Nd, and Pb isotope systematics. *Geology* **27**, 83–86.

Iwamori H. (1998) Transportation of H_2O and melting in subduction zones. *Earth Planet. Sci. Lett.* **160**, 65–80.

Jochum K. P. and Hofmann A. W. (1997) Constraints on earth evolution from antimony in mantle-derived rocks. *Chem. Geol.* **139**, 39–49.

Jochum K. P., Seufert H. M. and Thirlwall M. F. (1990) High-sensitivity Nb analysis by spark-source mass spectrometry (SSMS) and calibration of XRF Nb and Zr. *Chem. Geol.* **81**, 1–16.

John T., Scambelluri M., Frische M., Barnes J. and Bach W. (2011) Dehydration of subducting serpentinite: implications for halo-gen mobility in subduction zones and the deep halogen cycle. *Earth Planet. Sci. Lett.* **308**, 65–76.

Kendrick M. A., Scambelluri M., Honda M. and Phillips D. (2011) High abundance of noble gas and chlorine delivered to the mantle by serpentinite subduction. *Nat. Geosci.* **4**, 807–812.

King R., Bebout G. E., Moriguti T. and Nakamura E. (2006) Elemental mixing systematics and Sr-Nd isotope geochemistry of mélange formation: Obstacles to identification of fluid sources to arc volcanics. *Earth Planet. Sci. Lett.* **246**, 288–304.

King R., Bebout G. E., Grove M., Moriguti T. and Nakamura E. (2007) Boron and lead isotope signatures of subduction-zone melange formation: hybridization and fractionation along the slab–mantle interface beneath volcanic fronts. *Chem. Geol.*

Klein E. M. (2003) Geochemistry of the Igneous Oceanic Crust. Chapter 3.13: The Crust (eds. H. D. Holland and K. K. Turekian), Treatise on Geochemistry, pp. 433–463.

Kodolányi J., Pettke T., Spandler C., Kamber B. S. and Gmeling K. (2012) Geochemistry of ocean floor and fore-arc serpen-tinites: constraints on the ultramafic input to subduction zones. *J. Petrol.* **53**, 235–270.

Lafay R., Deschamps F., Schwartz S., Guillot S., Godard M. and Nicollet C. (2013) High-pressure serpentinites, a trap-and-release system controlled by metamorphic conditions: example from the Piedmont zone of the Western Alps. *Chem. Geol.* **343**, 38–54.

Leeman W. R. (1996) Boron and other fluid-mobile elements in volcanic arc lavas: implications for subduction process. In *Subduction: 'Top to Bottom', Am. Geophys. Union Geophys.*

Monogr., vol. 96 (eds. G. E. Bebout, D. W. Scholl, S. H. Kirby and J. E. Platt), pp. 269–276.

Li Y. H. (1991) Distribution patterns of the elements in the ocean – a synthesis. *Geochim. Cosmochim. Acta* **55**, 3223–3240.

Malatesta C., Crispini L., Federico L., Capponi G. and Scambelluri M. (2012) The exhumation of high pressure ophiolites (Voltri Massif, Western Alps): insights from structural and petrological data on metagabbri bodies. *Tectonophysics* **568–569**, 102–123.

Marschall H. R. and Schumacker J. C. (2012) Arc magmas sourced from mélange diapirs in subduction zones. *Nat. Geosci.* **5**, 862–867.

Marschall H. R., Ludwig T., Altherr R., Kalt A. and Tonarini S. (2006) Syros metasomatic tourmaline: evidence for very high-δ^{11}B fluids in subduction zones. *J. Petrol.* **47**, 1915–1942.

McDonough W. F. and Sun S. S. (1995) The composition of the Earth. *Chem. Geol.* **120**, 223–253.

Meyre C., De Capitani C. and Partzsch J. H. (1997) A ternary solid solution model fro omphacite and its application to geothermobarometry of eclogites from the Middle Adula nappe (Central Alps, Switzerland). *J. Metamorphic Geol.* **15**, 678–700.

Meyre C., De Capitani C., Zack T. and Frey M. (1999) Petrology of high-pressure metapelites from the Adula Nappe (Central Alps, Switzerland). *J. Petrol.* **40**, 199–213.

Mockel J. R. (1969) Structural petrology of the garnet peridotite of Alpe Arami (Ticino, Switzerland). *Leidse Geologische Medelingen* **42**, 61–130.

Moran A. E., Sisson V. B. and Leeman W. R. (1992) Boron depletion during progressive metamorphism: implications for subduction processes. *Earth Planet. Sci. Lett.* **111**, 331–349.

Mottl M. J., Komor S. C., Fryer P. and Moyer C. L. (2003) Deep-slab fuel extremophilic Archea on a Mariana forearc serpentinites mud volcano: Ocean Drilling Program Leg 195. *Geochem. Geophys. Geosyst.* **4**(11), doi:10.1029/2003GC000588.

Nagel T., De Capitani C. and Frey M. (2002) Structural and metamorphic evolution during rapid exhumation in the Lepontine dome (southern Simano and Adula nappes, Central Alps, Switzerland). *Eclogae Geol. Helv.* **95**, 301–321.

Nakano T. and Nakamura E. (2001) Boron isotope geochemistry of metasedimentary rocks and tourmaline in a subduction zone metamorphic suite. *Phy. Earth Planet. Int.* **127**(1), 233–252.

Nimis P. and Trommsdorff V. (2001) Revised thermobarometry of Alpe Arami and other garnet peridotites from the Central Alps. *J. Petrol.* **42**, 103–115.

Onishi H. and Sandell E. B. (1955) Geochemistry of arsenic. *Geochim. Cosmochim. Acta* **7**, 1–33.

Pabst S., Zack T., Savov I. P., Ludwig T., Rost D., Tonarini S. and Vincenzi E. P. (2012) The fate of subducted oceanic crust in the shallow mantle: insights from boron isotopes and light element composition of metasomatized blueschists from the Mariana forearc. *Lithos* **132–133**, 162–179.

Palmer M. R. and Swihart G. H. (1996) Boron isotope geochemistry: an overview. *Rev. Mineral.* **33**, 709–744.

Peacock S. M. (1993) Large-scale hydration of the lithosphere above subducting slabs. *Chem. Geol.* **108**, 49–59.

Peacock S. M. and Hervig R. L. (1999) Boron isotopic composition of subduction-zone metamorphic rocks. *Chem. Geol.* **160**, 281–290.

Pfiffner M. (1999) Genese der hochdruckmetamorphen ozeanischen Abfolge der Cima Lunga-Einheit (Zentralalpen). Ph. D thesis, ETH Zurich.

Pfiffner M. and Trommsdorff V. (1998) The high-pressure ultramafic-mafic-carbonate suite of Cima Lunga-Adula, Central Alps: excursions to Cima di Gagnone and Alpe Arami. *Schweiz. Mineral. Petrogr. Mitt.* **78**, 337–354.

Plank T. (2014) The chemical composition of subductin sediments. Chapter 4.17: The crust (ed. R. Carlson). *Treatise on Geochemistry*, second ed. pp. 607–629.

Rehkamper M. and Hofmann A. W. (1997) Recycled ocean crust and sediment in Indian Ocean MORB. *Earth Planet. Sci. Lett.* **147**, 93–106.

Ringwood A. E. (1974) The petrological evolution of island arc systems. *J. Geol. Soc. Lond.* **130**, 183–204.

Rosner M., Erzinger J., Franz G. and Trumbull R. B. (2003) Slab-derived boron isotope signatures in arc volcanic rocks from the Central Andes and evidence fro boron isotope fractionation during progressive slab dehydration. *Geochem. Geophys. Geosyst.* **4**, 9005.

Rudnick R. L. and Gao S. (2003) Composition of the continental crust. Chapter 3.01: the crust (eds. H. D. Holland and K. K. Turekian) *Treatise on Geochemistry*, pp. 1–64.

Ryan J. G., Chauvel C. (2014) The subduction zone filter and the impact of recycled materials on the evolution of the mantle. Chapter 3.13: The mantle and core (ed. R. Carlson). *Treatise on Geochemistry*, second ed. pp. 479–508.

Ryan J. G. and Langmuir C. H. (1993) The systematics of boron abundances in young volcanic rocks. *Geochim. Cosmochim. Acta* **57**, 1489–1498.

Ryan J. G., Morris J. D., Tera F., Leeman W. P. and Tsvetkov A. (1995) Cross-arc geochemical variations in the Kurile island arc as a function of slab depth. *Science* **270**, 625–628.

Ryan J. G., Leeman W. P., Morris J. D. and Langmiur C. H. (1996) Th boron systematics of intraplate lavas: implications for crust and mantle evolution. *Geochim. Cosmochim. Acta* **60**, 415–422.

Savov I. P., Ryan J. G., D'Antonio M., Kelley K. and Mattie P. (2005) Geochemistry of serpentinized peridotites from the Mariana Forearc Conical Seamount, ODP Leg 125: implications for elemental recycling at subduction zones. *Geochem. Geophys. Geosyst.* **6**, Q04J15.

Savov I. P., Ryan J. G., D'Antonio M. and Fryer P. (2007) *Shallow Slab Fluid Release Across and Along the Mariana Arc-Basin System: Insights from Geochemistry of Serpentinized Peridotites from the Mariana Fore Arc*. Geology Faculty Publications Paper, p. 8.

Scambelluri M. and Tonarini S. (2012) Boron isotope evidence for shallow fluid transfer across subduction zones by serpentinized mantle. *Geology* **40**, 907–910.

Scambelluri M., Muntener O., Hermann J., Piccardo G. B. and Trommsdorff V. (1995) Subduction of water into the mantle: history of an alpine peridotite. *Geology* **23**, 459–462.

Scambelluri M., Bottazzi P., Trommsdorff V., Vannucci R., Hermann J., Gomez-Pugnaire M. T. and Lopez-Sanchez Vizcaino. V. (2001) Incompatible element-rich fluids released by antigorite breakdown in deeply subducted mantle. *Earth Planet. Sci. Lett.* **192**, 457–470.

Scambelluri M., Muntener O., Ottolini L., Pettke T. and Vannucci R. (2004) The fate of B, Cl and Li in the subducted oceanic mantle and in the antigorite-breakdown fluids. *Earth Planet. Sci. Lett.* **222**, 217–234.

Scambelluri M., Pettke T., Rampone E., Godard M. and Reusser E. (2014) Petrology and trace element budgets of high-pressure peridotites indicate subduction dehydration of serpentinized mantle (Cima di Gagnone, Central Alps, Switzerland). *J. Petrol.* **55**, 459–498.

Schmid S. M., Pfiffner O. A., Froitzheim N., Schonnorn G. and Kissling E. (1996) Geophysical-geological transect and tectonic evolution of the Swiss-Italian Alps. *Tectonics* **15**, 1036–1064.

Schmid S. M., Fugenschuh B., Kissling E. and Schuster R. (2004) Tectonic map and overall architecture of the Alpine orogen. *Eclogae Geol. Helv.* **97**, 93–117.

Spandler C. and Pirard C. (2013) Element recycling from subducting slabs to arc crust: a review. *Lithos* **170–171**, 208–223.

Spandler C., Hermann J., Faure K., Mavrogenes J. A. and Arculus R. A. (2008) The importance of talc and chlorite "hybrid" rocks for volatile recycling through subduction zones: evidence from the high-pressure subduction mélange of New Caledonia. *Contrib. Mineral Petrol* **155**, 181–198.

Stampfli G. M., Mosar J., Marquer D., Marchant R., Baudin T. and Borel G. (1998) Subduction and obduction processes in the Swiss Alps. *Tectonophysics* **296**, 159–204.

Sun S. S. and McDonough W. F. (1989) Chemical and isotopic systematics of oceanic basalts; implications for mantle composition and processes. In *Magmatism in the ocean basins,* vol. 42, (eds. A. D. Saunders and M. J. Norry), Geological Society of London, London, pp. 313–345.

Syracuse E. M., van Keken P. and Abers G. A. (2010) The global range of subduction zone thermal models. *Phys. Earth Planet. Inter.* **183**, 73–90.

Todt W., Cliff R. A., Hanser A. and Hofmann A. W. (1993) Re-calibration of NBS lead standards using a ^{202}Pb–^{205}Pb double spike. *Terra Abstr.* **5**(1), 396.

Tonarini S., Leeman W. P. and Ferrara G. (2001) Boron isotopic variations in lavas of the Aeolian volcanic arc, South Italy. *Journal of Volcanology and Geothermal Research* **110**(1), 155–170.

Tonarini S., Pennisi M. and Leeman W. P. (1997) Precise boron analysis of complex silicate (rock) samples using alkali carbonate fusion and ion exchange separation. *Chem. Geol.* **142**, 129–137.

Tonarini S., Agostini S., Doglioni C., Innocenti F. and Manetti P. (2007) Evidence for serpentinite fluid in convergent margin systems: the example of El Salvador (Central America) arc lavas. *Geochem. Geophys. Geosyst.* **8**(9).

Tonarini S., Pennisi M., Adorni-Braccesi A., Dini A., Ferrara G., Gonfiantini R., Wiedenbeck M. and Gröning M. (2003) Intercomparison of boron isotope and concentration measurements: Part I: Selection, preparation and homogeneity tests of the intercomparison materials. *Geostand. Newslett.* **27**, 21–39.

Tonarini S., Agostini S., Innocenti F. and Manetti P. (2005) Δ^{11}B as tracer of slab dehydration and mantle evolution in Western Anatolia Cenozoic Magmatism. *Terra Nova* **17**, 259–264.

Tonarini S., Leeman L. W. and Leat P. T. (2011) Subduction erosion of forearc mantle wedge implicated in the genesis of the South Sandwich Island (SSI) arc: Evidence from boron isotope systematics. *Earth Planet. Sci. Lett.* **301**, 275–284.

Trommsdorff V. (1966) Progressive Metamorphose kieseliger Karbonatgesteine in den Zentralalpen zwischen Bernina und Simplon. *Schweiz. Mineral. Petrogr. Mitt.* **46**, 431–460.

Trommsdorff V. (1990) Metamorphism and tectonics in the Central Alps: the Alpine lithospheric mélange of Cima Lunga and Adula. *Mem. Soc. Geol. Ital.* **45**, 39–49.

Trommsdorff V., Hermann J., Muntener O., Pfiffner M. and Risold A. C. (2000) Geodynamic cycles of subcontinental lithosphere in the Central Alps and the Arami enigma. *J. Geodyn.* **30**, 77–92.

Associate editor: Clark M. Johnson